2-1-2010

Bond Performance of Sprayed Fire Resistive Material (SFRM) on Steel Plates Subjected to Tensile Loading

Nicole Leo Braxtan

Stephen Pessiki

Bond Performance of Sprayed Fire Resistive Material (SFRM) on Steel Plates Subjected to Tensile Loading

by

Nicole Leo Braxtan

Stephen Pessiki

ATLSS Report No. 10-01

February 2010

ATLSS is a National Center for Engineering Research on Advanced Technology for Large Structural Systems

117 ATLSS Drive
Bethlehem, PA 18015-4729

Phone: (610)758-3525
Fax: (610)758-5902

www.atlss.lehigh.edu
Email: inatl@lehigh.edu

Bond Performance of Sprayed Fire Resistive Material (SFRM) on Steel Plates Subjected to Tensile Loading

by

Nicole Leo Braxtan
Post-doctoral Research Associate
Department of Civil and Environmental Engineering

Stephen Pessiki
Professor and Chairperson
Department of Civil and Environmental Engineering

ATLSS Report No. 10-01

February 2010

ATLSS is a National Center for Engineering Research on Advanced Technology for Large Structural Systems

117 ATLSS Drive
Bethlehem, PA 18015-4729

Phone: (610)758-3525
Fax: (610)758-5902

www.atlss.lehigh.edu
Email: inatl@lehigh.edu

ACKNOWLEDGEMENTS

This research was supported by the Pennsylvania Infrastructure Technology Alliance (PITA) and by the Center for Advanced Technology for Large Structural Systems (ATLSS). Funding was also provided through the Gibson Fellowship, Yen Fellowship, Hoppes Fellowship, and Brinks Fellowship. Findings and conclusions are those of the authors and not of the sponsors.

TABLE OF CONTENTS

LIST OF TABLES

LIST OF FIGURES

ABSTRACT

Sprayed fire resistive material (SFRM) is an integral part of structural fire protection for multistory steel building construction. SFRM is intended to thermally protect structural steel elements during a fire. Damage to the SFRM can compromise the efficacy of the SFRM and lead to elevated temperatures in the steel substrate and thus a reduction in strength and stiffness of the steel.

The work presented in this report is part of a broader research program to evaluate the efficacy of sprayed fire resistive material in steel moment frame building structures in the event of a post-earthquake fire. The focus of this report is tensile plate tests to investigate the bond of SFRM to steel plates at various levels of post-yield strain in the plates.

Tests were performed to determine bond performance of SFRM on steel plates subjected to tensile yielding. SFRM was applied to a series of steel plates. The plates were then loaded in tension to various levels of strain above the yield strain. After loading, bond tests were performed on the SFRM to determine the adhesive and cohesive strengths of the SFRM. The tests results were interpreted to understand the degradation of bond strength as a function of strain level in the steel substrate.

Three variables were treated in the tests: (1) type of SFRM (dry-mix, portland cement and mineral wool fiber, and wet-mix, gypsum and vermiculite); (2) plate surface condition (mill scale and sandblasted); and (3) peak tension strain level in the plates.

When the SFRM materials treated in this research are applied to steel that has mill scale, the adhesive strength of the SFRM degrades rapidly once the steel yields. The rapid degradation of the adhesive strength is attributed to the debonding of the mill scale from the steel as the steel yields, coupled with the fact that the SFRM is bonded to the mill scale and not the underlying steel.

Both the dry-mix and the wet-mix SFRMs exhibit improved adhesive strength in loaded plates when the mill scale is removed by sandblasting prior to the application of the SFRM to the steel.

For the wet-mix SFRM treated in this research, the initial adhesive strength (i.e. the adhesive strength to an unloaded steel plate) increases if the mill scale is removed by sandblasting prior to the application of the SFRM.

CHAPTER 1
INTRODUCTION

1.1 INTRODUCTION

Current U.S. practice uses a combination of active and passive fire protection systems to provide structural fire protection in multistory building construction. Active fire protection systems include sprinklers, firefighters, automatic door closers, fire extinguishers, and fans or other devices used to control smoke. Passive fire protection systems are those built into the building system that do no require specific activation, such as sprayed fire-resistive materials (SFRMs). Sprinklers and other active systems are intended to extinguish a fire or to limit its spread, and SFRM is intended to thermally protect structural steel elements during a fire.

Past events have demonstrated that earthquakes can cause fires in buildings, damage active fire protection systems such as sprinklers, and reduce the effectiveness of fire-fighting capabilities. In such an event where the active fire protection systems are compromised by an earthquake, passive systems such as SFRM may be the only available means to mitigate the effects of the fire on the structural system in a building. However, during an earthquake, the integrity of the SFRM may become compromised because of damage to the underlying steel structure to which the SFRM is bonded. For example, for traditional strong-column weak-beam designs, large deformation demands are place on the beams in the vicinity of the columns, which in turn place large demands on the ability of the SFRM to remain attached to the beams. Lesser demands from the earthquake are placed on the column; thus the column SFRM may remain intact during the earthquake. Damage to the SFRM in the plastic hinge region in the beam adjacent to the column provides a means to conduct heat directly into the column in the event of a post-earthquake fire. Thus damaged SFRM may reduce the structural performance of the building columns at elevated temperature during a post-earthquake fire.

1.1.1 Research Objective

The work presented is this report is part of a broader research program to evaluate the efficacy of sprayed fire resistive material in steel moment frame building structures in the event of a post-earthquake fire. To date, the focus of the work has been on the axial load behavior of the steel column in a fire as influenced by damage to the SFRM in the beams adjacent to the columns.

1.1.2 Summary of Approach

The scope of this research includes four tasks.

- Task 1 – tensile plate tests to investigate the bond of SFRM to steel plates at various levels of post-yield strain in the plates.
- Task 2 – cyclic loading tests of beam-column assemblages with SFRM to determine earthquake induced patterns in the SFRM.
- Task 3 – nonlinear finite element heat transfer analyses to determine the fire-induced temperature distribution in the beam-column connection region due to damaged SFRM on the beam.

Task 4 – nonlinear finite element structural analyses of the strength of the columns, at the elevated temperatures determined in Task 3, due to fire and damaged SFRM.

This report addresses the results of Task 1. Task 1 includes the tensile plate tests performed to examine the cohesive and adhesive strength of SFRM to steel at varying levels of strain, including beyond yield. SFRM was applied to a series of steel plates. The plates were then loaded in tension to various levels of strain above the yield strain. After loading, bond tests were performed on the SFRM to determine the adhesive and cohesive strengths of the SFRM as influenced by the tension tests. The test results were interpreted to understand the degradation of bond strength as a function of strain level in the steel substrate.

1.2 ORGANIZATION OF REPORT

The remainder of this report is organized into four chapters (Chapters 2 through 5) that each discuss an important aspect of this research.

Chapter 2 presents the background information relevant to this research. The sprayed fire resistive materials studied in this research are described, and the existing ASTM methods for testing these materials are discussed. Chapter 3 presents the tensile plate tests that were performed to determine the damage to the bond of SFRM precipitated by yielding of the underlying steel to which the SFRM is bonded. Chapter 4 presents the results of the tensile plate tests and discusses the implications of these results. Chapter 5 presents the conclusions of this research.

1.3 SUMMARY OF FINDINGS

Two SFRM materials were treated in this research: (1) a dry-mix material (portland cement and mineral wool fibers); and (2) a wet-mix material (vermiculite and gypsum).

When the SFRM materials treated in this research are applied to steel that has mill scale, the adhesive strength of the SFRM degrades rapidly once the steel yields. The rapid degradation of the adhesive strength is attributed to the debonding of the mill scale from the steel as the steel yields, coupled with the fact that the SFRM is bonded to the mill scale and not the underlying steel.

The wet-mix SFRM has higher adhesive strength to steel than the dry-mix SFRM. Adhesive strength of the wet-mix SFRM on unloaded plates was about 3 times as great as the adhesive strength of the dry-mix SFRM on unloaded plates.

The wet-mix SFRM maintains bond to the steel at higher strain levels than the dry-mix SFRM. As was found in the visual inspections after the tension loading, the dry-mix SFRM tends to debond from the steel surfaces while the wet-mix SFRM cracked but maintained the bond. This affect was first seen at the edges of the SFRM after loading, but the concept holds true for the central portion of the plate where bond tests were performed.

Sandblasting of the steel plates helps maintain adhesive strength to the steel at higher strain levels. Plates that were not sandblasted still had mill scale on the surface and once yielding progressed over the plate, the mill scale fell off effectively eliminating the bond between the steel and the SFRM.

Sandblasting of the steel plate increases unloaded adhesive strength in the wet-mix SFRM but does not offer this same advantage in the dry-mix SFRM.

SFRM may become detached from the steel plate after loading beyond yield. Detachment of the SFRM was more prevalent in the plates sprayed with the dry-mix SFRM than in the plates sprayed with the wet-mix SFRM. The fibrous dry-mix SFRM tends to remain as one integral unit. When strains become large and strain compatibility at the interface of the dry-mix SFRM and the steel is lost, the dry-mix SFRM debonds from the surface of the steel.

SFRM may crack after loading beyond yield. Cracking occurred in the wet-mix SFRM but not in the dry-mix SFRM. When strains become large and strain compatibility at the interface of the steel becomes difficult to maintain, the cementitous wet-mix SFRM tends to crack to accommodate large deformations. The bond between the wet-mix SFRM and the steel is strong and the wet-mix SFRM tends to detach from the steel at a lesser extent than dry-mix SFRM does.

1.4 NOTATION

The following notation is used throughout this report.

A = area of the cap
CA = cohesive/adhesive force
F = recorded force
M = mass of the SFRM sample
V = volume of the SFRM sample
ρ = density of the SFRM

1.5 UNIT CONVERSIONS

Metric units are used consistently throughout this report. The following unit conversions can be used to convert to U.S. customary units.

1 kg/m^3= 6.24x10^{-2} lb/ft^3
1 mm = 25.4 in.
1 N = 2.25x10^{-1} lbf
1 Pa = 1.45x10^{-4} psi

CHAPTER 2
BACKGROUND

2.1 INTRODUCTION
This chapter presents the background information relevant to this research. The sprayed fire resistive materials (SFRMs) studied in this research are described, and the existing ASTM methods for testing these materials are discussed.

2.2 SPRAYED FIRE RESISTIVE MATERIAL
SFRM is used as a method of passive fire protection to thermally insulate structural steel elements during a fire. Figure 2.1 is a photograph of SFRM applied to typical beams and columns in a building under construction. Two commonly used SFRM materials are treated in this research: a dry-mix material and a wet-mix material. Both materials are briefly described below.

2.2.1 Sprayed Fire Resistive Material Description
The dry-mix material is a portland cement and mineral wool fiber mixture. The product is conveyed in the dry state under low air pressure and water is added at the spray nozzle as the product is being applied. This dry-mix material is referred to as DM in this paper.

The wet-mix material is a mixture of vermiculite and gypsum. It is combined with water in a large mixer before being pumped in a wet-slurry state to a spray nozzle where compressed air creates a spray pattern as the product is applied. It is predominantly sprayed but can be applied using a trowel. This wet-mix material is referred to as WM in this paper.

2.2.2 Test Methods for Sprayed Fire Resistive Material
Several test methods exist to evaluate the properties of SFRM. Of interest to this research are methods to evaluate the bond strength of SFRM to structural members, and the thickness and density of SFRM. This section of the report reviews ASTM E736: Standard Test Method for Cohesion/Adhesion of Sprayed Fire-Resistive Material (SFRM) Applied to Structural Members, and ASTM E605: Standard Test Methods for Thickness and Density of Sprayed Fire-Resistive Material (SFRM) applied to Structural Members.

2.2.2.1 ASTM E736: Standard Test Method for Cohesion/Adhesion of Sprayed Fire-Resistive Material (SFRM) Applied to Structural Members
This test method is used to evaluate the cohesive or adhesive strength of SFRM applied to structural members. A brief summary of the method is as follows. Specimens are prepared by applying 12 to 25 mm of SFRM to a 300 mm by 300 mm galvanized steel plate or field testing is performed on structural members with existing SFRM. A bottle cap with a hook inserted into it, similar to that shown in Figure 2.3, is filled with a two-component glue and placed on the SFRM surface. After the glue has cured, a spring type scale is attached to the hook and force is applied, pulling on the cap until the SFRM fails.

Failure within the SFRM is classified as a cohesive failure and failure between the SFRM and the steel surface is classified as an adhesive failure. The maximum force is recorded from the scale and the bond strength is determined based on the force and the area of the cap.

$$CA = \frac{F}{A} \tag{2.1}$$

where

CA = cohesive/adhesive force, Pa
F = recorded force, N
A = area of the cap, m^2

2.2.2.2 ASTM E605: Standard Test Methods for Thickness and Density of Sprayed Fire-Resistive Material (SFRM) Applied to Structural Members

As the name suggests, this test method is used to determine the thickness and density of SFRM on structural members. Test specimens are prepared by applying SFRM to a 1.5 mm thick, bare or galvanized steel plate that is 400 mm by 400 mm in area, or field testing is performed on structural members with existing SFRM. Thickness measurements are taken at 12 locations on the plate, or member, and an average thickness is found based on these results. The thickness is found by inserting a pin through the SFRM until it reaches the steel substrate. The pin includes a scale that measures the depth of penetration from the surface of the SFRM to the steel substrate.

The density of the SFRM is then determined as follows. A 5800 mm^2 sample of SFRM is cut from the plate, or member, and the mass determined using a scale. The volume of the SFRM is then found using the displacement method described in the standard. The density is calculated as

$$\rho = \frac{m \cdot 1000}{V} \tag{2.2}$$

where

ρ = density of the SFRM, kg/m^3
M = mass of the sample, g
V = volume of the sample, cm^3

Figure 2.1 – Photograph of sprayed fire resistive material in building

(a) (b)

Figure 2.2 – Photograph of wet-mix and dry-mix materials: (a) cementitious wet-mix material; and (b) fibrous dry-mix material

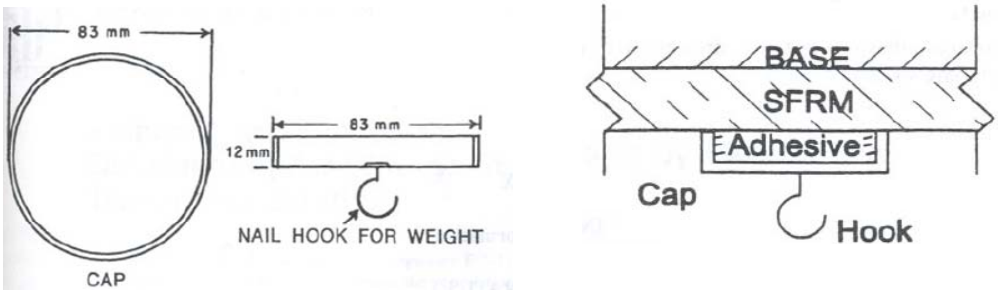

Figure 2.3 – Cap used in ASTM E736 for bond testing (ASTM E736, 2000)

CHAPTER 3
TENSILE PLATE TEST SET-UP

3.1 INTRODUCTION

This chapter presents the tests that were performed to determine the damage to the bond of SFRM precipitated by yielding of the underlying steel to which the SFRM is bonded. SFRM was applied to a series of steel plates. The plates were then loaded in tension to various levels of strain above the yield strain. After loading, bond tests were performed on the SFRM to determine the adhesive and cohesive strengths of the SFRM as influenced by the tension tests. The tests results were interpreted to understand the degradation of bond strength as a function of strain level in the steel substrate.

Three variables were treated in the tests: (1) type of SFRM (dry-mix or wet-mix); (2) plate surface condition (mill scale or sandblasted); and (3) peak tension strain level in the plates. Results are discussed in terms of SFRM bond strength degradation as a function of increasing steel strain and steel surface preparation. Temperature and relative humidity were recorded during testing to track environmental changes and density and thickness of the SFRM for each sample were determined for completeness.

3.2 SPRAYED FIRE RESISTIVE MATERIALS TESTED

As explained in Chapter 2, two commonly used commercial types of SFRM were used in this testing: a dry-mix material (DM) and a wet-mix material (WM).

Application of the SFRM to the steel plates was performed by the manufacturer's technicians at their laboratory. After the application of the SFRM, the plates were left to cure for six weeks before they were carefully moved back to the testing facilities at Lehigh University for the tensile and bond testing. Figure 3.1 shows the DM dry materials in the applicator, Figure 3.2 shows the manufacturer's technician preparing for the application of DM, and Figure 3.3 shows the DM applicator with a separate water jet. The WM was applied with a single spray nozzle as the WM is mixed with water prior to application. The WM mixer and applicator are shown in Figure 3.4. Further details of the SFRM application process are presented in Chapter 5.

3.3 TEST MATRIX

Table 3.1 shows the test matrix for the tensile plate testing. A total of twenty-eight plates were included in the test matrix and twenty-four plates were subject to tensile loading. Fourteen plates were sprayed with DM and fourteen plates were sprayed with WM. Seven of the plates for each material were sandblasted prior to SFRM application to remove the mill scale and the other seven were cleaned to remove dirt and oil with an all-purpose household cleaner, leaving the mill scale intact.

Plates are identified as either "M" or "SB" for plates with mill scale (not sandblasted) and plates sandblasted to remove mill scale, respectively. The letter following this indicates the individual plate being tested. For example, DM-M-A indicates Plate A of the DM, mill scale plates.

Four additional 1.5 m long plates (not shown in the table), one for each representative plate group, not subjected to tension tests, were used to determine the bond strength of unloaded plates as well as to track any changes in bond strength due to environmental changes over the duration of testing.

All plates were A36 steel. The mill certification for the steel plates is given in Appendix A.2. Tension tests confirmed that the yield stress of the plates was approximately 329 MPa, approximately 1% higher than the 325 MPa yield stress reported in the Mill Certification.

3.4 PLATE GEOMETRY AND INSTRUMENTATION

In this section the side of the plate with the SFRM is referred to as the "front" face and the other side is referred to as the "back" face.

Figure 3.5 shows the test plate geometry and instrumentation. Each test specimen is comprised of a steel plate that measures approximately 1.1 m long by 152 mm wide by 6 mm thick. The central 457 mm of the front face of the plate had SFRM applied, leaving 305 mm on each end bare to allow for gripping during the tension tests. Six 12.7 mm gage length strain gages were used for each test specimen. One gage was centered on each face, at the center of the plate, and one gage was centered at each of the four test locations on the back face. The gages were consistently numbered on the test plates as follows. Gage 1 was centered on the front face of the plate, and Gage 6 was centered on the back face. Gages 2 through 6 were located on the back side of the plate with Gage 2 in the upper left corner, Gage 3 in the upper right corner, Gage 4 in the lower left corner, and Gage 5 in the lower right corner. The two centered gages (Gage 1 and Gage 6) were applied to record an average overall strain, and to track any bending in the plate. Gage 1 on the front face of the plate was protected during SFRM application with silicon rubber, Teflon, and waterproofing.

Gages 1 and 6 were intended to control the loading to meet the target strain levels presented in the test matrix. Preliminary test plates had only these two gages, but the variation in local strain over the testing area was great. Therefore, four additional gages were included on the actual test plates to track the local strains at each test location. The actual strain levels achieved at each test location (Gage 2 through 5) during testing were different from the target strain levels previously discussed and are tabulated in Chapter 4 with the bond test results.

3.5 TENSION TESTS

All tensile testing was performed using a 2669 kN (600 kip) capacity universal testing machine at the ATLSS Center Laboratory. Figure 3.6 shows the test machine and Figure 3.7 shows a typical plate specimen installed in the test machine.

All plates were loaded in displacement control. A loading rate of 1.27 mm per minute was used in each test. Strain gages were wired to a signal conditioner and data was recorded through a general data acquisition program. Both the conditioner and the data

acquisition system are shown in Figure 3.8. Strains were recorded from the strain gages and the load and head travel data was recorded directly from the test machine.
For each test, each plate was loaded past yield until the gages were near the target strain values and then unloaded back to zero load. After tensile testing of the plates was complete, the plates were carefully removed from the test machine and prepared for bond testing.

3.6 BOND TESTS

The bond tests were performed in the test fixture shown in Figure 3.9. The test fixture was comprised of a self-reacting test frame, hand-operated mechanical actuator, load cell, and data acquisition system. The plate specimen under test was clamped to the lower beam of the test frame as shown in Figure 3.9. The test fixture had a hand crank jack suspended from the upper beam. The jack was attached to a load cell used to read the applied force.

Square blocks of 19 mm thick plywood were glued to each of the test locations using a two-component polyurethane glue. The blocks were pre-drilled with holes at the center that were used to insert screw hooks during testing. These hooks were then used to attach the testing block to the load cell and jack mounted to the test frame.

Figure 3.10 shows the preparation of the specimens for bond testing. Part (a) shows the specimen laid out with four wooden test blocks and parts A and B of the two component glue. Part (b) shows the combining of the two glue parts on the wooden block. As the two parts mix together the glue begins to expand rapidly. The blocks are then firmly held down on the SFRM to ensure they remain parallel to the steel surface, shown in Part (c). Once the wood blocks were glued to the SFRM, the excess glue was wiped away before it cured or carefully cut away after curing. The glue was left to dry for a minimum of four hours to ensure proper curing. Each block was then cut from the surrounding material to eliminate any influence of nearby test blocks or any shear resistance in the SFRM during testing, as seen in Part (d). Part (e) shows a test specimen ready for testing.

Each steel plate with test blocks glued on was clamped to the lower beam of the test frame to prevent upward flexing of the plate during testing (see Figure 3.11). To perform the actual bond test, the hand crank on the jack was turned, inducing a small upward motion on the block, as shown in Figure 3.11. ASTM E736 recommends a minimum loading rate of 0.8 N/sec, but does not specify a maximum loading rate. As a practical matter with the hand crank, the actual rate of loading was approximately 2.2 N/sec. The force that the material resisted against this upward pull was recorded through the load cell and the data acquisition system. The data acquisition system included signal conditioners and a multimeter, as shown in Figure 3.12. A multimeter was used to record the maximum voltage output during each test. Voltage was converted to load through a calibration constant, and the load was then used along with the area of the SFRM below the block to determine the bond strength of the material. The calibration is shown in Figure 3.13.

When failure occurred, the actual area of SFRM on the block was carefully calculated since this area varied slightly from block to block or because during the cutting process the cuts were not exactly straight. The force determined from the voltage output divided by the area of SFRM gave the adhesive bond strength. The actual strain under the block was known from the strain gage mounted at each location on the opposite side of the plate, and the resulting bond strength of the material at that particular strain was recorded.

Six different modes of failure were observed during the bond testing as shown in Figure 3.14. Stage 1 shows the wood blocks being set up prior to testing. Stage 2 shows the different failure modes observed during testing. Part (a) of the figure shows adhesive failure between the steel plate and the SFRM. This was the desired type of failure during testing. Part (b) shows cohesive failure within the SFRM. Part (c) shows a combination of both cohesive failure within the SFRM and adhesive failure between the steel and the SFRM. Part (d) shows cohesive failure of the glue when the glue broke and part (e) shows adhesive failure at the interface of the glue and wood block. These two types of glue failure may have been due to proportioning error when mixing the two-component glue. Part (f) shows failure of the wooden block itself when the layers of the plywood pulled apart.

If cohesive failure occurred, a new block was glued to the newly exposed SFRM surface and tested again until adhesive failure occurred. If the failure was a combination of adhesive and cohesive failure, retesting could not be performed since there was now a portion of exposed, bare steel. If failure occurred in the wood or the glue, appropriate measures where taken to retest the material including replacing the wooden block with a new block.

3.7 DENSITY AND THICKNESS TESTING

Density and thickness testing was performed on each plate in accordance with ASTM E605: Standard Test Methods for Thickness and Density of Sprayed Fire-Resistive Material (SFRM) Applied to Structural Members (2000). That standard was reviewed in Chapter 2.

3.8 ENVIRONMENTAL TESTING

Temperature and relative humidity were recorded throughout the duration of testing to track any environmental changes. The recorder was placed in the lab near the bond testing fixture and continually recorded during the months of testing. When the relative humidity was very high, testing was not performed due to curing problems with the glue. The effect of temperature was not apparent in the bond test results, and discussion of the potential effect of relative humidity is presented in Chapter 4.

Table 3.1 – Tensile plate target test matrix

SFRM Material		DM		WM	
Surface Condition		Mill Scale	Sandblasted	Mill Scale	Sandblasted
Target Peak Tension Strain (multiple of ε_y)	0	DM-M-0	DM-SB-0	WM-M-0	WM-SB-0
	1	DM-M-A	DM-SB-A	WM-M-A	WM-SB-A
	2	DM-M-B	DM-SB-B	WM-M-B	WM-SB-B
	4	DM-M-C	DM-SB-C	WM-M-C	WM-SB-C
	6	DM-M-D	DM-SB-D	WM-M-D	WM-SB-D
	8	DM-M-E	DM-SB-E	WM-M-E	WM-SB-E
	10	DM-M-F	DM-SB-F	WM-M-F	WM-SB-F

Figure 3.1 – DM dry materials in applicator

Figure 3.2 – Technician ready to apply DM

Figure 3.3 – DM applicator with separate water jet

Figure 3.4 – WM mixer and applicator

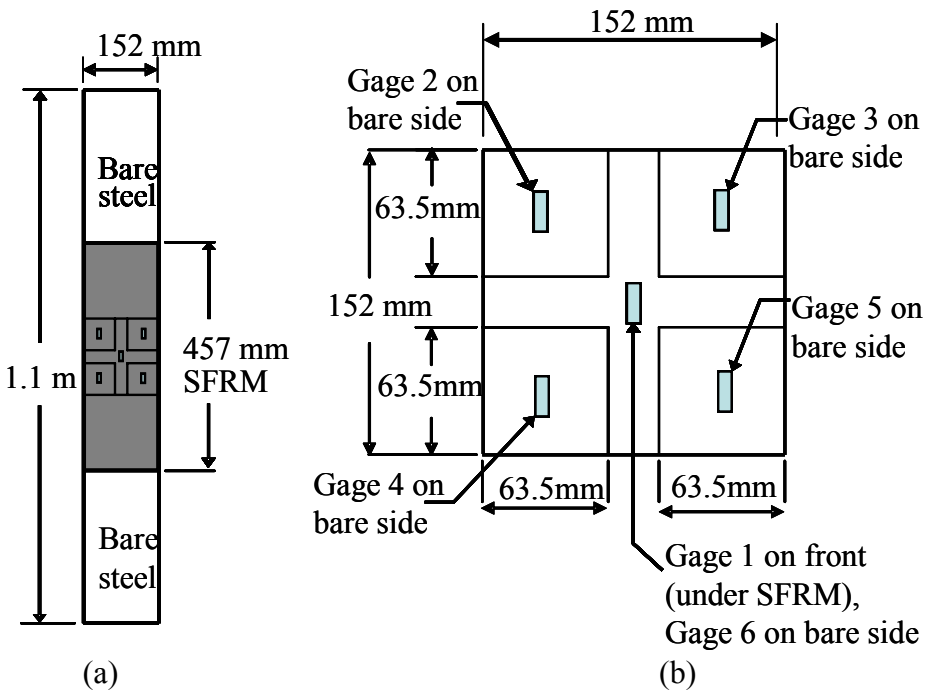

Figure 3.5 – Test plate setup: (a) overall view of test plate; and (b) close-up of test area (note front face is the side of the plate with the SFRM)

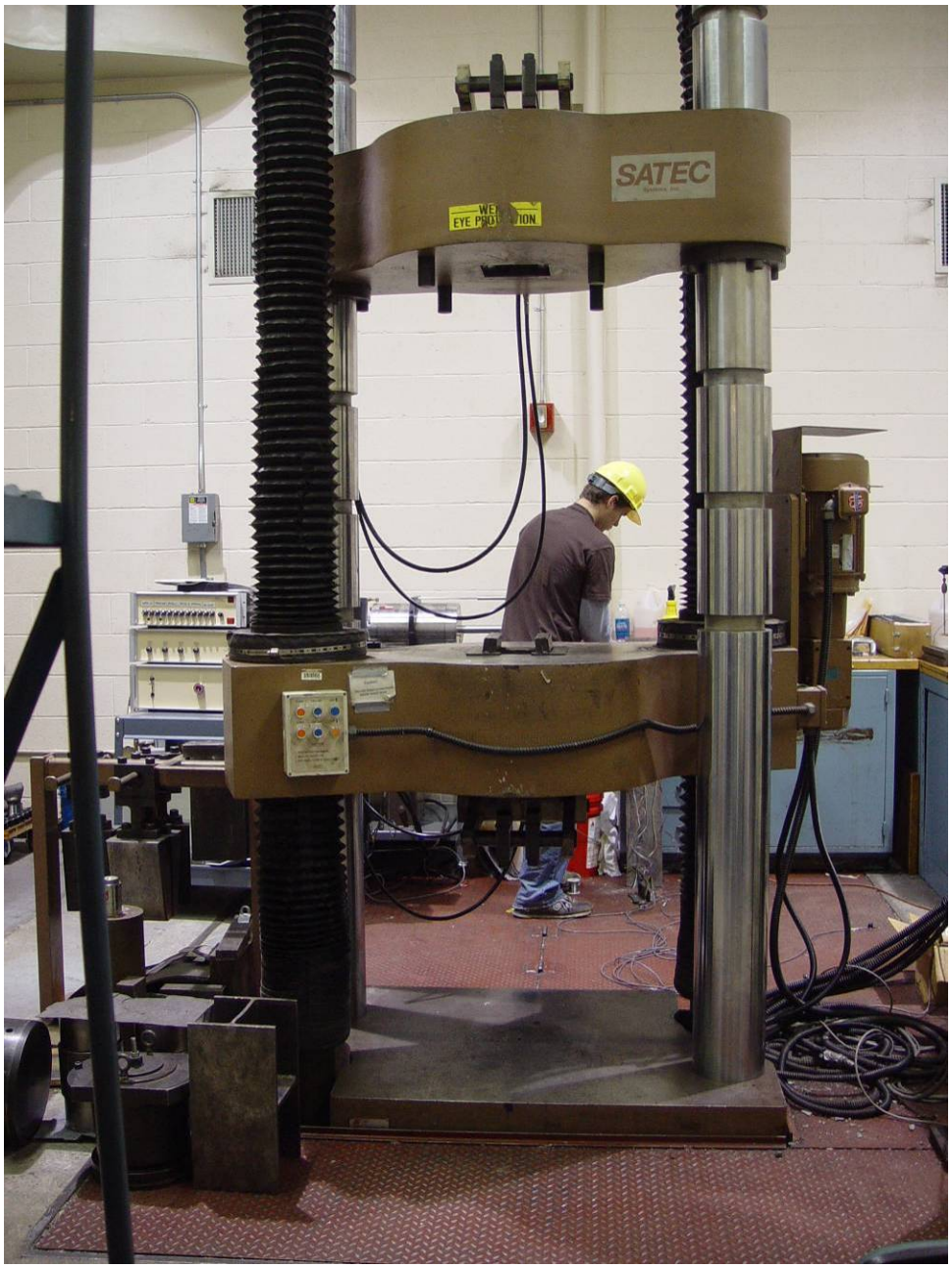

Figure 3.6 – Universal testing machine

Figure 3.7 – Plate specimen installed in universal testing machine

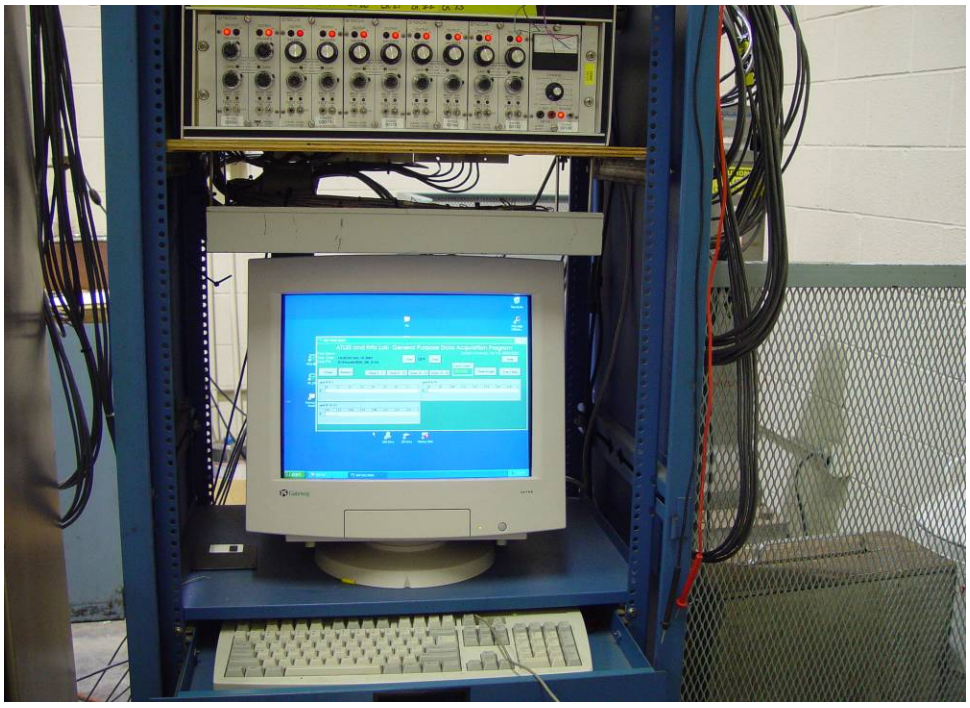

Figure 3.8 – Signal conditioner and data acquisition system

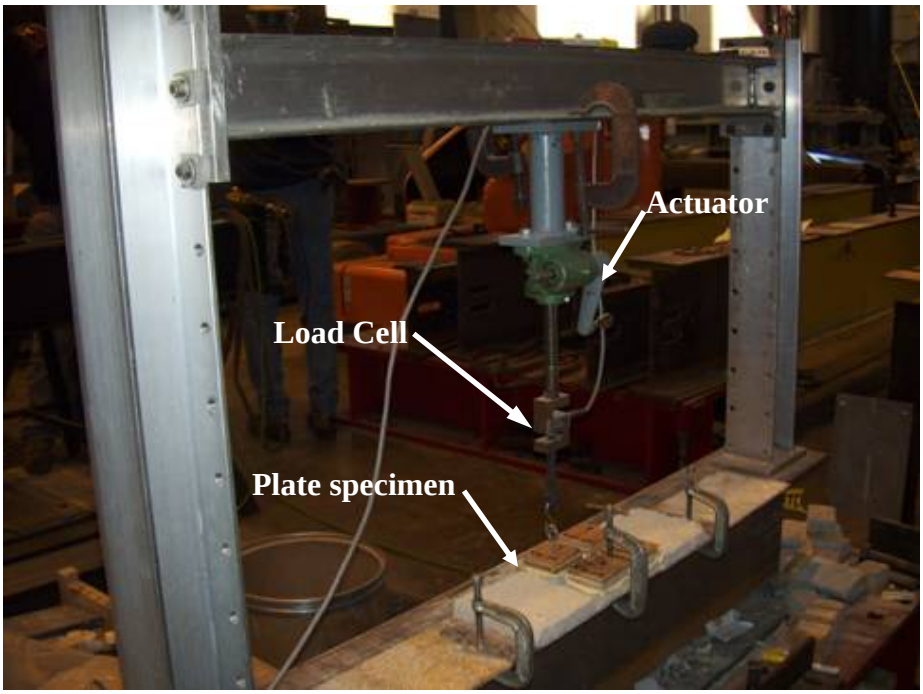

Figure 3.9 – Test frame used for bond testing shown with plate specimen clamped in place for testing

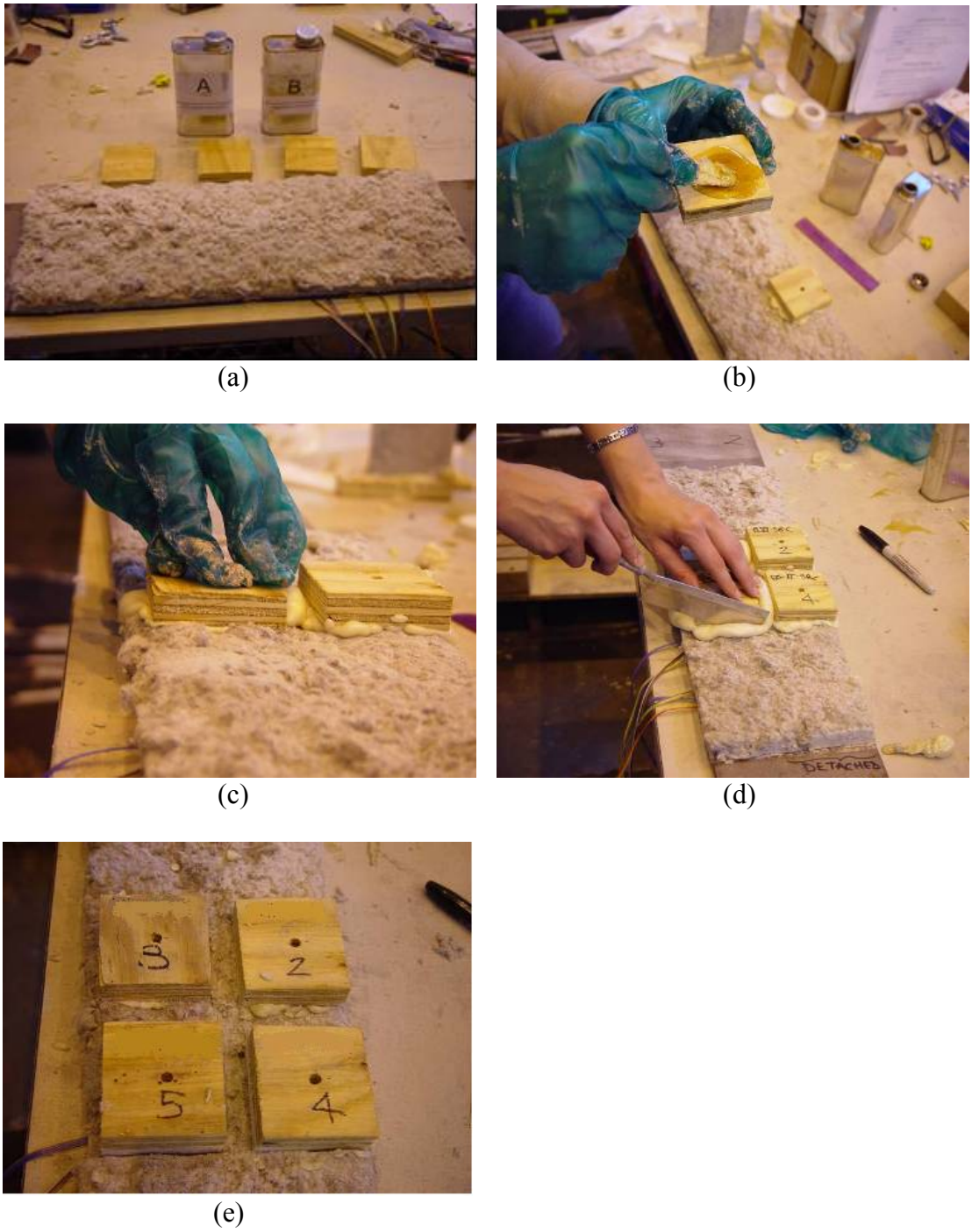

(a) (b) (c) (d) (e)

Figure 3.10 – Preparing specimen for bond testing: (a) specimen with test blocks and A and B glue; (b) combining A and B glue; (c) glue expands as it cures; (d) cutting around each test block; and (e) test blocks labeled and ready for testing

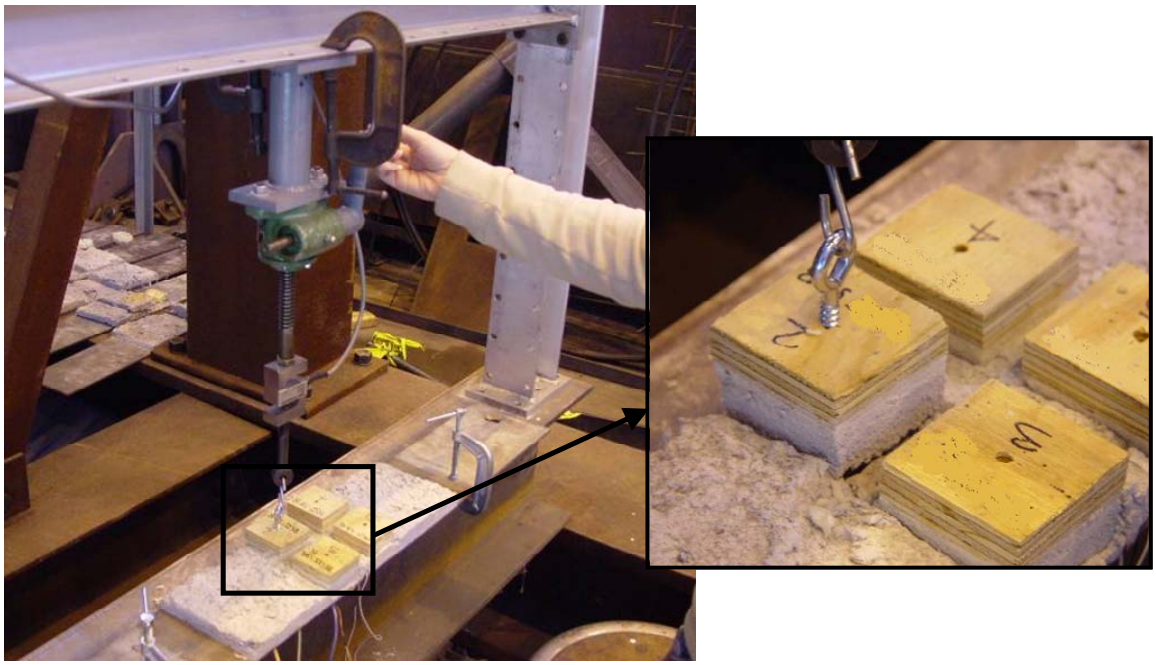

Figure 3.11 – Load applied to test block, enlarged view of adhesive failure

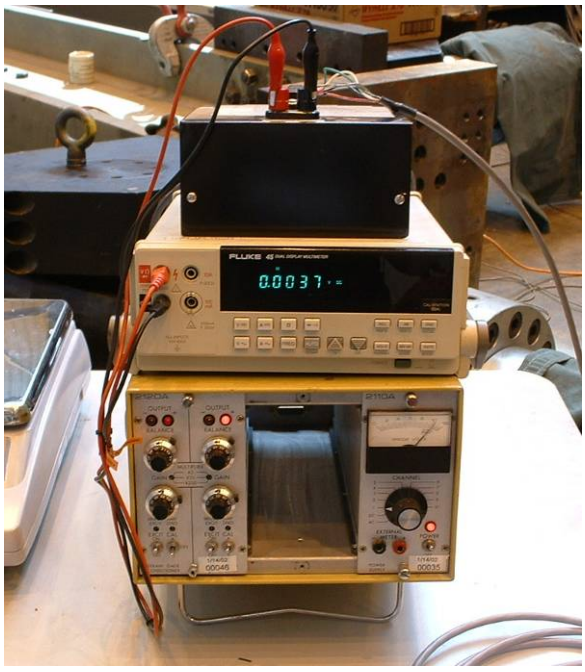

Figure 3.12 – Multimeter and signal conditioner for bond testing

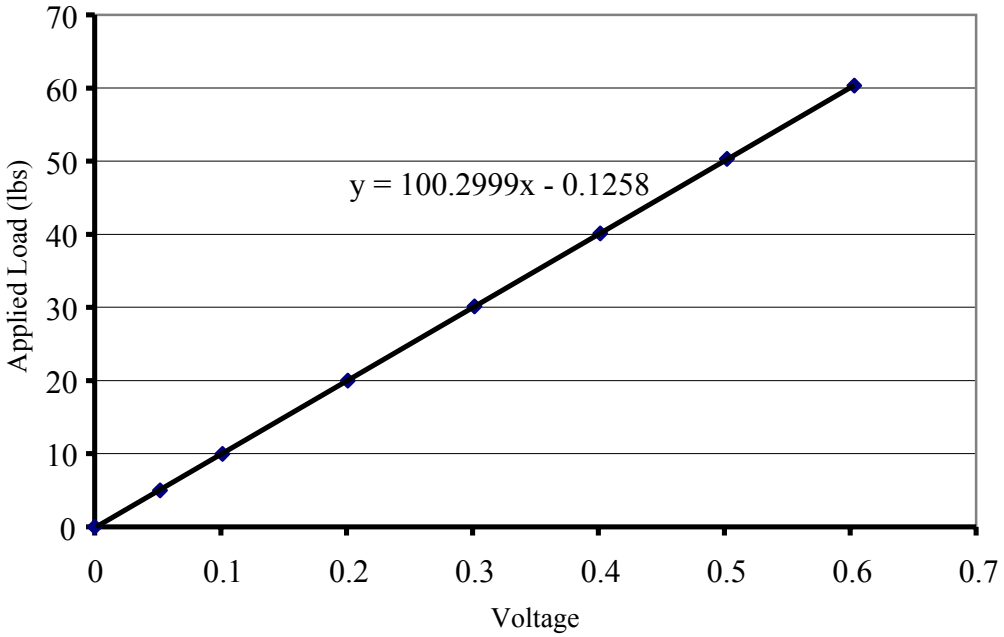

Figure 3.13 – Load cell calibration for tensile plate tests

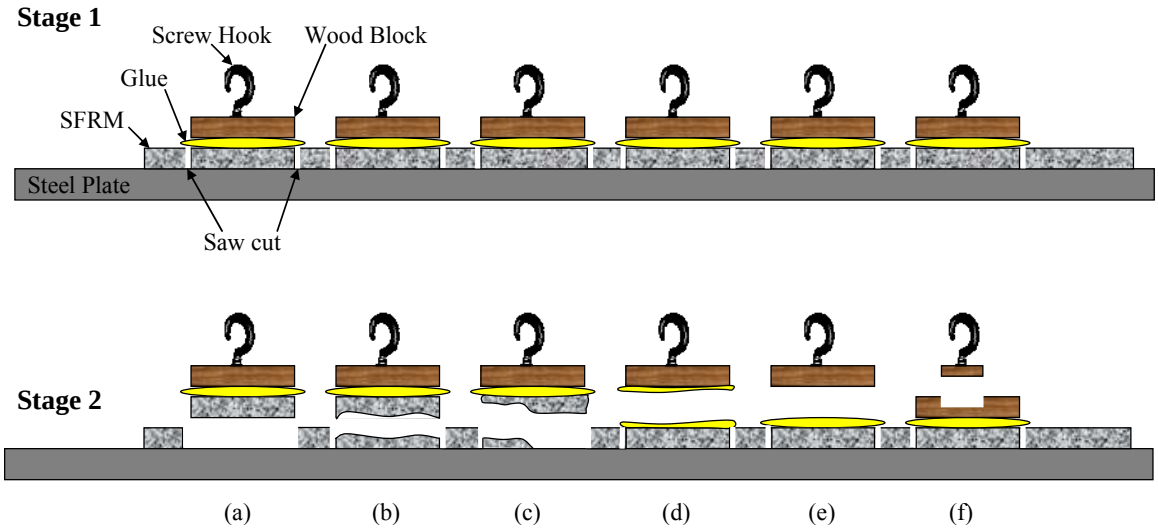

Figure 3.14 – Possible modes of failure during bond tests: (a) adhesive failure; (b) cohesive failure; (c) combined adhesive and cohesive failure; (d) glue failure (e) adhesive failure at the interface of the glue and the block; and (f) wood block failure

CHAPTER 4
TENSILE PLATE TEST RESULTS AND DISCUSSION

4.1 INTRODUCTION
This chapter presents the results of the tensile plate tests and discusses the implications of these results.

4.2 RESULTS
Tension loading results are given in terms of typical stress-strain behavior and maximum strain at bond test locations. Bond test results are presented in terms of bond strength and failure type.

4.2.1 Tension Loading Results
Stress-strain data from the loading of a typical plate is shown in Figure 4.1. Data is shown for Gages 2, 3, 4, and 5 (centered on the test block locations) to illustrate the variation in strain between each test location. The x-axis shows strain in the steel plate at the test locations. Each increment on the graph is equal to one multiple of the expected yield strain (ε_y) of the steel plate for easier comparison. Only every other increment is labeled such that the first labeled increment of 0.0032 is 2 times the yield strain ($2 \cdot \varepsilon_y$). Stress-strain data for plate WM-SB-F is shown in Figure 4.2; this was the only plate that exhibited strain hardening.

4.2.2 Bond Test Results
Maximum strains in the steel and the final adhesive strength for each test location are shown in Table 4.1. The multiple of yield strain associated with these strains is also shown in brackets in the table. Zero bond strength was reported when the SFRM was detached from the steel prior to bond testing. For all instances of zero bond strength the sample being tested became separated from steel when the first cut was made into the material.

For completeness, Table 4.2 shows the bond strength and failure type for all bond tests, including the final adhesive strength. Adhesive failure is noted as "A." Cohesive failure is noted as "C." Combined adhesive and cohesive failure is noted as "A/C." Failure within the glue itself is noted as "G," failure at the glue/block interface is noted as "I", and failure of the wooden block itself is noted as "W." Any failure that occurred during cutting of the SFRM was noted as "cut."

Multiple bond tests were attempted for some of the test locations on many of the plates as cohesive, or other types of failures, occurred prior to the final adhesive failure. Figure 4.3 shows the failure strength of SFRM for each consecutive bond test performed at each location on plate WM-M-D. Only one bond test was required at the location of Gage 2. Five bond tests were performed at the location of Gage 5, and the failure strength increased with each trial. Six bond tests were performed at the location of Gage 4, and in all but the second trial there was an increase in the failure strength. Gage 3 shows an example where the final adhesive strength is lower than at least one of the previous tests,

and the failure strength is not consistently increasing with each trial. This is one particular plate example, but similar charts could be produced for all plates based on the information shown in Table 4.2.

Graphical results for the bond tests are shown in Figure 4.4 through Figure 4.7. Final adhesive strength, or combined adhesive and cohesive strength if failure occurred in that manner, is plotted on the y-axis. Any prior cohesive, glue, or wood failures are not shown here for brevity since the desired result was adhesive strength.

The strain of the underlying steel at each test location is plotted on the x-axis. Each increment is equal to one multiple of the expected yield strain (ε_y) of the steel plate for easier comparison. Only every other increment is labeled such that the first labeled increment of 0.0032 is 2 times the yield strain ($2 \cdot \varepsilon_y$).

Each graph shows the minimum acceptable bond strength of 7.2 kPa (150 psf) as reported in the manufacturer's guide specifications in accordance with General Services Administration AIA/SC/GSA/07811. Each graph also shows and the value obtained from laboratory tests performed by the manufacturer as per ASTM E736. For DM the tested value is 17.2 kPa and for WM the tested value is 18.8 kPa. It is noted that the ASTM E736 does not distinguish between cohesive and adhesive failures.

4.2.2.1 Unloaded Plate Results

Table 4.3 shows the failure type and bond strength for all of the unloaded plate tests. The unloaded DM-M and DM-SB plates had a range of adhesive strengths with averages similar to the manufacturer's tested values. Unloaded DM-M plates had an average adhesive strength of 16.3 kPa and unloaded DM-SB plates had an average adhesive strength of 14.9 kPa compared to 17.2 kPa for the manufacturer's tested values. The wide range of these values is indicative of the non-homogenous nature of DM as the dry-mix materials for DM tend to coalesce together unevenly. Also, when the DM is applied it is sprayed in layers building up to the desired thickness causing some areas to be compacted more than others.

The unloaded WM-M plates had an average adhesive strength of 43.1 kPa and the unloaded WM-SB plates had an average adhesive strength of 54.8 kPa compared to the manufacturer's tested value of 18.8 kPa. For most of the WM unloaded bond tests, there were several cohesive failures prior to the final adhesive failure. The difference in the manufacturer's tested value and the average adhesive strength determined in this research is assumed to be attributed to the ASTM considering the cohesive or adhesive strength of the material and the research presented here considering the final adhesive strength.

4.2.2.2 Dry-mix Results

Figure 4.4 and Figure 4.5 show the variation of adhesive strength with strain of the underlying steel of the DM plates. The unloaded plate bond strengths are similar for both the DM-M and the DM-SB. The DM-M plates show a rapid reduction in adhesive strength as the steel strain increases. By the point in each figure where the steel strain is

at yield strain, the adhesive strengths fall below the minimum accepted value. For the samples just beyond yield strain there was a complete loss of adhesive strength. These test blocks were completely detached from the steel after the test blocks were cut from the surrounding areas. This was the case for 5 different test blocks at steel strains of 1.5 times the yield strain and beyond.

The DM-SB plates were able to maintain adhesive strength for higher strain values, although these values fell well below the accepted strength of 7.2 kPa. Tests performed for locations that were at strain levels approaching 2 times yield were greater than the minimum acceptable strength. For bond tests done at locations with steel strain between 2 and 10 times the yield strain there was minimal adhesive strength. However, the only bond test that showed zero adhesive strength after cutting was at a strain level about 11.5 times the yield strain.

4.2.2.3 Wet-mix Results

Figure 4.6 and Figure 4.7 show the adhesive strength of WM as the strain in the underlying steel is increased. Both the WM-M and the WM-SB unloaded plates had much higher bond strength values than the DM plates and also much higher than the tested values. Adhesion for the WM plates is maintained at higher strains than the DM plates as the strain in the steel increases. In fact the WM-M plates still met the standard value at about 5.5 times the yield strain and the WM-SB plates were still acceptable at 12 times the yield strain. This finding is in agreement with findings from visual inspection after loading of the plates when it was found that the WM bond was well maintained and cracking occurred in lieu of detachment of the SFRM from the steel.

4.3 DISCUSSION OF RESULTS

Results are discussed in two sections: (1) results involving the loading portion of the testing; and (2) results from the bond strength testing.

4.3.1 Crack and Detachment of Sprayed Fire Resistive Material

Two important characteristics were found after the plates were loaded in tension: (1) detachment of the SFRM from the steel plates; and (2) cracking of the SFRM. Table 4.4 summarizes the occurrences of cracking and detachment in the plates.

Large portions of SFRM became detached from the steel plate before any cutting was performed for the bond tests in some of the DM plates. This detachment occurred at the top or bottom edges of the SFRM. Figure 4.8 show this occurrence on one of the DM-M plates, DM-M-A. Part (a) shows the bottom 127 mm of SFRM that became detached during loading and part (b) shows that once the first cut was made into the material, the DM came off in one large piece. Plate DM-M-A had the highest average strain on the plate and was the only DM-M plate that had detachment at the ends. Two of the DM-SB plates also had detachment at the ends, DM-SB-C and DM-SB-E. These two plates had higher average strains over each plate. Two of the WM-M plates had detachment at the ends, but none of the WM-SB plates exhibited detachment.

Cracking of the SFRM perpendicular to the direction of loading occurred in all of the plates sprayed with WM, both sandblasted and not sandblasted. Examples of cracking are shown in Figure 4.9 where the cracks have been highlighted with marker for easier identification. Part (a) shows a typical WM-M plate that exhibited horizontal cracking at midheight of the SFRM. Each WM-M plate had one full width horizontal crack approximately at mid-length of the SFRM and a partial width crack between 38 mm and 63 mm away from the main crack. The WM-SB plates also exhibited this approximate midheight full width crack. However, some of the WM-SB plates had additional cracking. Part (b) shows plate WM-SB-C with additional minor cracking. Part (c) shows plate WM-SB-F that exhibited extensive cracking. This plate was the only plate that was loaded into the early stages of strain hardening and had the highest average strains of all the plates. Cracking was not observed in any of the DM plates, sandblasted or not sandblasted.

Cracking and detachment together help to illustrate the effect of strain compatibility between two materials. If the SFRM remains fully attached to the steel plate, then the SFRM and the steel must both have the same strain at the interface between the two. As strains get large, this strain compatibility can no longer be met. Either the SFRM cracks to accommodate the large strains and deformations or the SFRM slips from the steel below and becomes detached.

The DM plates did not exhibit visually observable cracking. This is due to both the fibrous nature of the material itself and the weaker bond between the DM and the steel. It is possible that the fibrous nature of the DM better distributed the cracking making it harder to observe visually. When strains were larger in the DM plates, detachment of the SFRM occurred at the edges. The DM-SB plates seemed to maintain the bond between the SFRM and the steel at higher strains than the DM-M plates. Plate DM-SB-A did not exhibit detachment and was loaded to an average strain near 5 times yield strain whereas plate DM-M-A showed detachment and had an average strain of only 3.6 times the yield strain.

As mentioned previously, all of the WM plates exhibited cracking. This is due to both the cementitous nature of the material and the greater bond between the WM and the steel. As the strains became larger in the steel plates the WM tended to remain bonded to the steel. In order to accommodate the large deformations and allow for the continued bond to the steel the WM cracked. More extensive cracking was seen in plates with higher average strains and the most extensive cracking was seen in the plate with the maximum average strain. Plates WM-M-A and WM-M-B also both showed detachment, but had the lowest average strains of the WM-M plates.

4.3.2 Bond Test Discussion

Recall Figure 4.4 through Figure 4.7 as the bond tests are discussed. Figure 4.4 and Figure 4.5 show that the DM-SB plates maintained higher adhesive strength than the DM-M plates. Figure 4.6 and Figure 4.7 show that the WM-SB plates maintained adhesive strength at higher strains than the WM-M plates. The WM-M plates had

diminished adhesive strength at around 8 to 10 times the yield strain with zero adhesive strength at approximately 10 time yield strain. Whereas the WM-SB plates had acceptable adhesive strength at strains nearly 12 times the yield strain.

Figure 4.6 and Figure 4.7 show that the WM-SB plates had higher adhesive strength in the unloaded plates than the WM-M plates. This is contrasted by the DM-M and DM-SB plates, shown in Figure 4.4 and Figure 4.5, which started at about the same unloaded plate adhesive strength where only the rate of adhesive strength lost differed. The sandblasting in the WM plates had a greater effect than sandblasting in the DM plate.

When considering the average values on each plate the trends become clearer. Figure 4.10 shows the average adhesive strength on each plate plotted against the average steel strain in each plate. Unloaded plate data is weighted for groups of four data points to allow for proper comparison with the four test blocks averaged on each loaded plate. Again the strain axis is incremented for multiples of yield strain. Linear trendlines have been added for each data set and the trendlines for WM-M and WM-SB have been extrapolated to zero adhesive strength as is shown with the dashed line.

Sandblasting of the plates increases the ability to maintain adhesive strength in the plates. The plates that were not sandblasted still had a layer of mill scale on them. As the steel plates yield, the mill scale falls off effectively eliminating the bond between the steel and the SFRM. Figure 4.11 shows some examples of plates that were not sandblasted and the resulting yield lines and loss of mill scale. Part (a) shows plate WM-M-A that exhibited detachment of the SFRM at the top, yielding progressing from the top of the plate downward, and a resulting diagonal band of yielding where mill scale had fallen off. Note that there is mill scale attached to the SFRM that has fallen off. Part (b) and (c) show plates WM-M-C and DM-M-D with diagonal yield lines and loss of mill in the central region of the plates where yielding progressed from and compares this effect between both materials. For the DM plates sandblasting approximately doubled the amount of strain that could be experienced before loss of adhesive strength. For the WM plates, if the trendlines were extrapolated to zero adhesive strength, there could be an increase of more than 2.5 times the amount of strain that could be experienced before loss of adhesive strength.

The WM plates showed an increase in the unloaded plate bond strength of about 25% when the plates were sandblasted whereas the DM plates were about the same. Sandblasting not only removed the mill scale but also roughened the surface on the steel plate. It is possible that the wet-mix WM had more of a propensity to fill in the irregular surface and better grasp onto the steel plates with its finer particles. The fibrous DM with larger portions of amalgamated materials may not have been able to initially benefit from the roughened surface.

The WM plates had approximately 3 times the initial unloaded bond strength than the DM plates. This is due to differences in the SFRM themselves. The fibrous, portland

cement based DM does not bond as well to the steel plates as the cementitous, gypsum based WM.

4.3.3 Density and Thickness Discussion

Figure 4.12 shows the average thickness of the SFRM on each plate plotted against the density of the SFRM. In general, the thinner the SFRM, the denser it was. The SFRM was applied in many passes, and it is likely that the material became more compacted as additional layers were applied.

The WM samples had a higher density than the DM samples and both materials had higher densities than what was reported in the manufacturer's literature. The results of density testing provided an average density of DM of 290 kg/m^3 compared to a minimum accepted density of 240 kg/m^3 as per UL standards and 256 kg/m^3 tested by the manufacturer. The average density for the WM in this testing was 407 kg/m^3, whereas the literature reported a minimum acceptable density of 240 kg/m^3 and a tested value of 280 kg/m^3. There was a larger difference between the reported "tested" density and the experimental density in the WM than the difference in the DM. The experimental density of the WM was about 45% higher than the tested density for WM while the experimental density of the DM was only about 13% higher than the tested density for DM. This difference could be attributed to a more deliberate and careful application process for this set of testing.

4.3.4 Environmental Discussion

Three factors were tracked on the unloaded plates to investigate any changes in material due to time, relative humidity, and temperature. Figure 4.13 shows the adhesive strength over time Figure 4.14 shows the cohesive strength over time to track any changes due to long term curing of the materials. Figure 4.15 and Figure 4.16 show the adhesive and cohesive strengths, respectively, plotted against the relative humidity recorded for the time of testing. Figure 4.17 and Figure 4.18 show the adhesive and cohesive strength, respectively, plotted against the temperature recorded at the time of testing

There were no significant trends found in the temperature tests. However, there seems to be a decrease in bond strength with increasing relative humidity in the WM plates. The trend is more visible in the cohesive strength tests in Figure 4.16 due to the larger number of tests. The DM plates showed no change in adhesive or cohesive strength with increasing relative humidity.

Curing of the material was tracked by recording the adhesive and cohesive strengths of the unloaded plates over time. No significant trends were seen in either the DM or WM plates, which indicates that the materials had fully cured when testing began. The earliest tests performed on the DM plates occurred 2 months after application of the SFRM. The earliest tests of the WM plates were done about 3.5 months after application of the SFRM.

4.4 SUMMARY OF FLATE PLATE TESTS

When the SFRM materials treated in this research are applied to steel that has mill scale, the adhesive strength of the SFRM degrades rapidly once the steel yields. The rapid degradation of the adhesive strength is attributed to the debonding of the mill scale from the steel as the steel yields, coupled with the fact that the SFRM is bonded to the mill scale and not the underlying steel.

WM has higher adhesive strength to steel than DM. Adhesive strength of WM on unloaded plates was about 3 times as great as the adhesive strength of DM on unloaded plates.

WM maintains bond to the steel at higher strain levels than DM. As was found in the visual inspections after the tension loading, the DM tend slip from the steel surfaces while WM cracked but maintained the bond. This affect was first seen at the edges of the SFRM after loading, but the concept holds true for the central portion of the plate where bond tests were performed.

Sandblasting of the steel plates helps maintain adhesive strength to the steel at higher strain levels. Plates that were not sandblasted still had mill scale on the surface and once yielding progressed over the plate, the mill scale fell off effectively eliminating the bond between the steel and the SFRM.

Sandblasting of the steel plate increases unloaded adhesive strength in WM but does not offer this same advantage in DM. As a possible explanation, the finer particles in the WM are able to benefit from the roughened surface caused by sandblasting. The fibrous DM's larger bundles of material cannot fill in the small ridges and valleys on the sandblasted surface so there is not a benefit to the unloaded adhesive strength.
SFRM may become detached from the steel plate after loading beyond yield. Detachment of the SFRM was more prevalent in the plates sprayed with DM than in the plates sprayed with WM. The fibrous DM tends to remain as one integral unit. When strains become large and strain compatibility at the interface of the DM and the steel is lost, the DM slips at the surface of the steel.

SFRM may crack after loading beyond yield. Cracking occurred in WM but not in the DM. When strains become large and strain compatibility at the interface of the steel becomes difficult to maintain, the cementitous WM tends to crack to accommodate large deformations. The bond between the WM and the steel is strong and WM tends to detach from the steel at a lesser extent than DM does.

For well-designed, strong column – weak beam moment frame steel structures in earthquakes, it is likely that steel yielding will first occur under the action of an earthquake causing story drifts of about 1%. Considering that debonding is a form of damage to the SFRM, damage to the SFRM will therefore begin under the action of an earthquake in well-designed steel moment frame structures. This damage will occur when the structure is in the early stages of the life safety level of performance.

Table 4.1 – Maximum strains in all plates and final adhesives strength for each test location

Plate	Maximum Strain in Each Gage (mm/mm) [Yield Multiple]				Final Bond Strength (kPa)			
	Gage 2	Gage 3	Gage 4	Gage 5	Gage 2	Gage 3	Gage 4	Gage 5
DM-M-A	0.001660 [1.0]	0.001700 [1.0]	0.003369 [2.1]	0.01681 [10.4]	2.5	5.3	0	0
DM-M-B	0.001753 [1.1]	0.001692 [1.0]	0.002351 [1.4]	0.003592 [2.2]	7.9	6.5	0	0
DM-M-C	0.001765 [1.1]	0.001619 [1.0]	0.002079 [1.3]	0.002185 [1.3]	6.6	9.9	3.1	9.4
DM-M-D	0.002433 [1.5]	0.001749 [1.1]	0.001668 [1.0]	0.007047 [4.3]	4.1	5.1	8.4	0
DM-M-E	0.000826 [0.5]	0.000826 [0.5]	0.000842 [0.5]	0.000858 [0.5]	13.9	19.1	19.4	18.6
DM-M-F	0.001794 [1.1]	0.001684 [1.0]	0.001656 [1.0]	0.001725 [1.1]	7.5	13.0	6.4	12.9
DM-SB-A	0.012992 [8.0]	0.006005 [3.7]	0.011079 [6.8]	0.001851 [1.1]	1.9	2.0	1.0	0.4
DM-SB-B	0.002587 [1.6]	0.003072 [1.9]	0.001684 [1.0]	0.001896 [1.2]	10.6	19.2	16.3	11.3
DM-SB-C	0.002286 [1.4]	0.001631 [1.0]	0.015840 [9.8]	0.008231 [5.1]	7.8	11.8	1.3	1.1
DM-SB-D	0.000830 [0.5]	0.000923 [0.6]	0.000830 [0.5]	0.000878 [0.5]	16.1	14.4	8.8	17.8
DM-SB-E	0.015083 [9.3]	0.009240 [5.7]	0.003649 [2.2]	0.01878[11.6]	0.3	2.1	3.2	0
DM-SB-F	0.005383 [3.3]	0.005159 [3.2]	0.001615 [1.0]	0.001664 [1.0]	1.9	2.3	15.5	12.8
WM-M-A	0.015157 [9.3]	0.001611 [1.0]	0.001611 [1.0]	0.001619 [1.0]	3.2	30.5	34.0	25.5
WM-M-B	0.001810 [1.1]	0.007771 [4.8]	0.006587 [4.1]	0.001777 [1.1]	29.8	4.9	14.1	37.5
WM-M-C	0.003076 [1.9]	0.001708 [1.1]	0.008768 [5.4]	0.015592 [9.6]	17.2	27.5	14.4	0.8
WM-M-D	0.013505 [8.3]	0.006640 [4.1]	0.002294 [1.4]	0.001761 [1.1]	1.4	12.1	46.8	43.3
WM-M-E	0.002294 [1.4]	0.001794 [1.1]	0.006249 [3.8]	0.012617 [7.8]	21.4	35.7	6.9	4.1
WM-M-F	0.001708 [1.1]	0.007462 [4.6]	0.016096 [9.9]	0.001770 [1.1]	37.7	11.3	0	17.3
WM-SB-A	0.004394 [2.7]	0.007718 [4.8]	0.001749 [1.1]	0.001717 [1.1]	34.6	31.4	33.7	40.1
WM-SB-B	0.002880 [1.8]	0.006665 [4.1]	0.006579 [4.1]	0.00312 [1.9]	53.0	34.8	51.7	52.5
WM-SB-C	0.001741 [1.1]	0.001684 [1.0]	0.010449 [6.4]	0.009769 [8.6]	52.1	54.2	41.3	44.6
WM-SB-D	0.014017 [8.6]	0.001603 [1.0]	0.009143 [5.6]	0.013793 [8.5]	36.5	30.0	34.6	42.4
WM-SB-E	0.016019 [9.9]	0.003072 [1.9]	0.012536 [7.7]	0.014872 [9.2]	31.7	42.5	40.4	28.7
WM-SB-F	0.019307[11.9]	0.018143 [11.2]	0.018554[11.4]	0.01868 [11.5]	26.4	16.2	11.4	14.8

Table 4.2 – Failure strength and type for all bond tests on loaded plates

Gage	Bond Strength (kPa)	Failure Type
DM-M-A		
2	2.5	A
3	5.3	A
4	0	Cut
5	0	Cut
DM-M-B		
2	7.9	A
3	6.5	A
4	0	Cut
5	0	Cut
DM-M-C		
2	6.6	A
3	9.9	A
4	3.1	A
5	9.4	A
DM-M-D		
2	4.1	A
3	5.1	A
4	8.4	A
5	0	Cut
DM-M-E		
2	13.9	A
3	19.1	A
4	13.7	C
	13.5	C
	19.4	A
5	17.7	C
	18.6	A
DM-M-F		
2	7.5	A
3	13	A
4	6.4	A
5	12.9	A
DM-SB-A		
2	1.9	A
3	2	A
4	1	A
5	0.4	A

Gage	Bond Strength (kPa)	Failure Type
DM-SB-B		
2	10.6	A
3	10.4	C
	8.2	C
	19.2	A
4	11.2	I
	13.5	C
	11.6	C
	16.3	A
5	11.3	A
DM-SB-C		
2	7.8	A
3	11.8	A
4	1.3	A
5	1.1	A
DM-SB-D		
2	7	C
	5.3	C
	8.7	C /I
	16.1	A
3	10.9	C
	12.9	C
	14.4	A
4	5.7	C
	8.5	C
	8.8	A
5	8.7	C
	9.3	C
	9.1	C
	17.8	A
DM-SB-E		
2	0.3	A
3	2.1	A
4	3.2	A
5	0	Cut
DM-SB-F		
2	1.9	A
3	2.3	A
4	10.6	C
	15.5	A
5	11	C
	12.8	A

Gage	Bond Strength (kPa)	Failure Type
WM-M-A		
2	3.2	A
3	9.6	I
	30.5	A
4	31.7	C/I
	33.4	C
	45.8	I
	6.2	C
	15	C
	34	A
5	12.3	I
	17.3	C
	16.7	C
	28.8	C
	25.5	A
WM-M-B		
2	8.6	I
	13.7	I
	14.1	I
	31.8	C
	29.8	A
3	4.9	A
4	14.1	A
5	37.5	A
WM-M-C		
2	17.2	A
3	11.9	C
	11.5	I
	29.4	C
	30.4	C
	30.9	C
	29.1	C
	21.6	C
	7.4	C
	27.5	A
4	3.8	I
	14.4	A
5	0.8	A

Table 4.2 – Failure strength and type for all bond tests on loaded plates [continued]

Gage	Bond Strength (kPa)	Failure Type
WM-M-D		
2	1.4	A
3	9.3	C
	5.7	C
	3.4	C/I
	21.6	C
	19	C
	12.6	C
	23.1	C
	12.1	A
4	15.5	C
	14	C
	25.6	C/I
	37.5	C
	45.1	C
	46.8	A
5	8.5	C
	16.7	C
	22.6	C
	32.9	C
	43.3	A
WM-M-E		
2	21.4	A
3	39.3	C
	37.3	C
	31.1	C
	19.5	C
	26.1	C
	22.6	C
	35.7	A/C
4	6.9	A
5	4.1	A
WM-M-F		
2	37.7	A
3	11.3	A
4	0	Cut
5	17.3	A/C

Gage	Bond Strength (kPa)	Failure Type
WM-SB-A		
2	34.6	A/C
3	39.1	C
	23.9	C
	31.4	A/C
4	52.2	C
	28.4	C
	26.3	C
	28.2	C
	33.7	A/C/G
5	40.1	A/C
WM-SB-B		
2	53	A/C
3	36.6	C
	27.7	C
	34.8	A/C
4	51.7	A/C
5	52.5	A/C
WM-SB-C		
2	40.6	W
	63.7	W
	19.6	C
	42.5	C
	35.5	C
	35.5	C
	24.4	C
	52.2	C
	38	C
	43.9	C
	33.8	G
	48.4	C
	52.1	A/C
3	54.2	A/C
4	41.3	A
5	44.6	A

Gage	Bond Strength (kPa)	Failure Type
WM-SB-D		
2	36.5	A/C
3	39.5	G
	20.5	C
	10.6	C
	25.4	C
	40.4	C
	25.3	C
	30	A/C
4	32.3	C
	26.5	C
	20.7	C
	35.3	C
	15.2	C
	34.6	A/C
5	15.6	C
	42.4	A/C
WM-SB-E		
2	31.7	A
3	39.3	C
	42.2	C
	42.5	A/C
4	35.9	W
	40.4	A/C
5	28.7	A/C
WM-SB-F		
2	26.4	A
3	16.2	A
4	11.4	A
5	14.8	A

Table 4.3 – Failure strength and type for all bond tests on unloaded plates

Block ID	Bond Strength (kPa)	Failure Type
DM-M		
A1	7.1	C
	13.2	I
	10	A
A2	11.9	C
	11.4	I
	16.2	A
A3	9.9	A
A4	17.7	A
A5	11.2	C
	16.5	A
A6	13.7	A
A7	13.5	C
	20.7	I
	11.1	C
	28.2	C
	22.7	A
A8	21.2	C
	18.7	A
A9	27.8	C
	24.6	C
	14.8	C
	20	A
A10	13.9	A
A11	15.4	C
	23.8	C
	16.6	A
A12	14.5	C
	12.5	C
	16.1	A
A13	10.3	I
	30.4	C
	17	C
	31	C
	23.8	C
	24.4	A
A14	29.2	C
	24.1	A/C
A15	3.7	C
	9.8	A
A16	25.6	A/C
A17	20.4	A
A18	8.7	C
	16.4	A
A19	17.2	C
	10.9	A

Block ID	Bond Strength (kPa)	Failure Type
A20	10.2	A
A21	14.6	C
	16.6	C
	20.8	C
	18.4	A
A22	8.8	C
	13.7	A
A23	9.5	A
A24	10	A
DM-SB		
A1	9.9	C
	13.1	C
	13.1	A
A2	11.9	C
	14.7	C
	12.3	C
	16.2	A
A3	8.8	I
	11.6	A
A4	10	C
	11.7	C
	11.5	I
	14.2	I
	21.4	A
A5	6	C
	13.4	C
	16.7	A
A6	2.5	C
	3.4	C/I
	13.6	A
A7	1.6	C
	11.2	A
A8	12.6	C
	12.1	A
A9	15.8	C
	21.7	A
A10	7.6	C
	9.4	C
A10	19.1	A
A11	11.7	C
	16.6	C
	15.2	A
A12	7.7	C
	9.8	C
	12.3	A
A13	9.4	A

Block ID	Bond Strength (kPa)	Failure Type
A14	7.4	C
	13	c
	14	A
A15	13.5	C
	16.5	C
	16.1	A
A16	18.7	C
	15.4	A
WM-M		
A1	10.9	C
	32.3	C
	21.8	C
	24.4	C
	51.3	C
	4.7	C
	17.5	I
	49.7	C
	34	A/C
A2	36.2	C
	27.2	C
	14.9	C
	24.4	C
	25.3	C
	1.6	C
	48.4	A
A3	29.6	C
	29.5	C
	12.6	C
	41.4	C
	15.6	C
	35.5	A
A4	27.3	C
	27.6	C
	25.4	C
	52.6	C
	4.9	C
	27.5	C
	27.4	I
	31.9	C
	12.5	I
	33.2	A
A5	6.5	C/I
	15.3	C
	25.8	C
	8.2	I
	40	A

Table 4.3 – Failure strength and type for all bond tests on loaded plates [continued]

Block ID	Bond Strength (kPa)	Failure Type
A6	8.7	C
	22.7	C
	28.7	C
	33.1	C
	51.2	A/C
A7	27.7	C
	13.2	C
	26.6	C
	36.6	C
	22.3	C
	35.5	C
	29.7	A
A8	3.8	I
	20.1	C
	21.4	C
	57.1	A
A9	30	C
	19.6	C
	31.6	A/C
A10	36.3	C
	26	C
	57.7	C
	45.6	G
	41.1	A/C
A11	17.9	C
	38.3	C
	52.5	C
	53.4	C
	46.3	G/I
	59.2	C
	63.4	G/C/I/A
A12	19.2	C
	36.9	A
A13	33.1	C
	40	C
	51.5	C
	59.1	A/C
A14	26.1	C
	35.6	C
	54.6	A
A15	24.5	C
	29.2	C
	36.3	C
	32.2	A/C
A16	30.4	C
	38.8	C

Block ID	Bond Strength (kPa)	Failure Type
A16	42.4	C/A
WM-SB		
A1	15.5	I
	42.7	C
	59.9	C
	24.4	C
	22.8	I
	25.7	C
	48.6	C
	57.5	I
A2	49.7	C
	49.3	C
	28.6	C
	28.7	C
	55.6	A
A3	42.8	A
A4	35.8	I
	38.1	I
	60.8	C
	9.4	C
	25.8	C
	47.3	C
	36.9	C
	52.6	C
	65.8	A
A5	21.7	C
	26.3	C
	38.3	C
	47.3	C
	39.8	C
	40.5	C
	34.1	A/C
A6	36.9	C
	17.3	C
	26	C
	32.3	C
	33	C
	45.1	C
	35.5	I
	36.1	C
	60.2	A/C
A7	12	C
	12.1	C
	23.6	C
	31.6	C
	28.8	C

Block ID	Bond Strength (kPa)	Failure Type
A7	65	C
	56.6	C
	69.4	A/C
A8	19.2	C
	14.8	C
	25.8	C
	27.6	C
	43.5	C
	37.3	C
	58.8	A
A9	28.6	C
	17.6	C
	46.4	C
	45.3	C
	52.6	A/C
A10	27	C
	17.4	C
	50.3	C
	45.1	C
	26.5	C
	41.7	C
	32.7	C
	56.9	A/C
A11	25.6	C
	35.3	C
	35.5	C
	45.1	C
	45.2	A/C
A12	25.3	C
	35.7	C
	41.5	C
	55.4	C
	58.3	A/C

Table 4.4 – Detachment and cracking occurrences

Plate ID	Average Strain	Detachment	Cracking
DM-M-A	$3.6\varepsilon_y$	Yes	No
DM-M-B	$1.4\varepsilon_y$	No	No
DM-M-C	$1.2\varepsilon_y$	No	No
DM-M-D	$2.0\varepsilon_y$	No	No
DM-M-E	$0.5\varepsilon_y$	No	No
DM-M-F	$1.0\varepsilon_y$	No	No
DM-SB-A	$4.9\varepsilon_y$	No	No
DM-SB-B	$1.4\varepsilon_y$	No	No
DM-SB-C	$4.3\varepsilon_y$	Yes	No
DM-SB-D	$0.5\varepsilon_y$	No	No
DM-SB-E	$7.2\varepsilon_y$	Yes	No
DM-SB-F	$2.1\varepsilon_y$	No	No
WM-M-A	$3.1\varepsilon_y$	Yes	Yes
WM-M-B	$2.7\varepsilon_y$	Yes	Yes
WM-M-C	$4.5\varepsilon_y$	No	Yes
WM-M-D	$3.7\varepsilon_y$	No	Yes
WM-M-E	$3.5\varepsilon_y$	No	Yes
WM-M-F	$4.1\varepsilon_y$	No	Yes
WM-SB-A	$2.4\varepsilon_y$	No	Yes
WM-SB-B	$3.0\varepsilon_y$	No	Yes
WM-SB-C	$3.6\varepsilon_y$	No	Yes
WM-SB-D	$5.9\varepsilon_y$	No	Yes
WM-SB-E	$7.2\varepsilon_y$	No	Yes
WM-SB-F	$11.5\varepsilon_y$	No	Yes

*Average strain computed as the strain at (Gage 2 + Gage 3 + Gage 4 + Gage 5) / 4

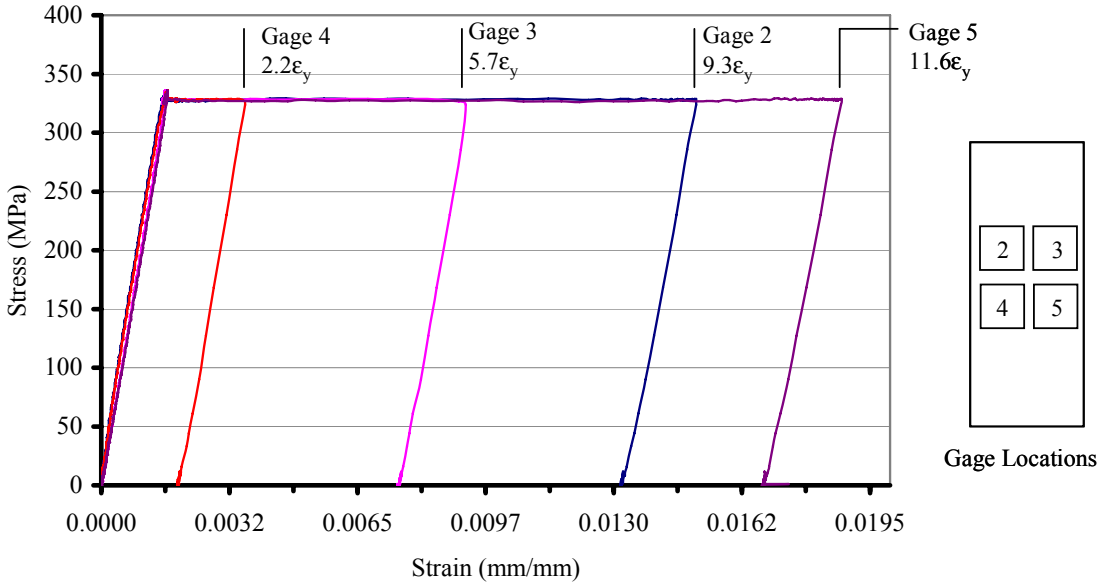

Figure 4.1 – Stress vs. strain data for test locations from a typical plate (DM-SB-E)

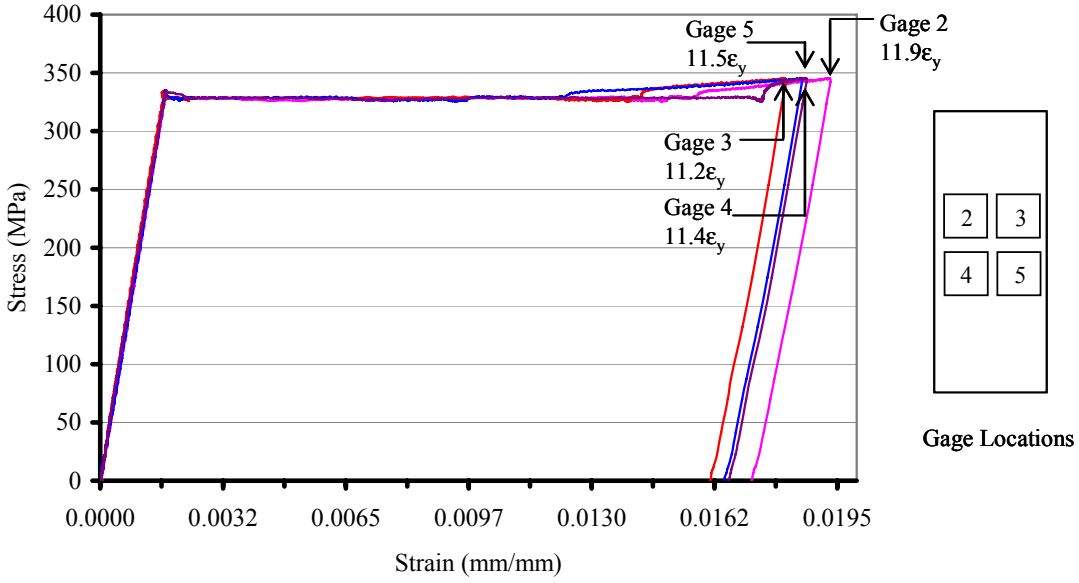

Figure 4.2 – Stress vs. strain for test locations on a plate showing strain hardening (WM-SB-F)

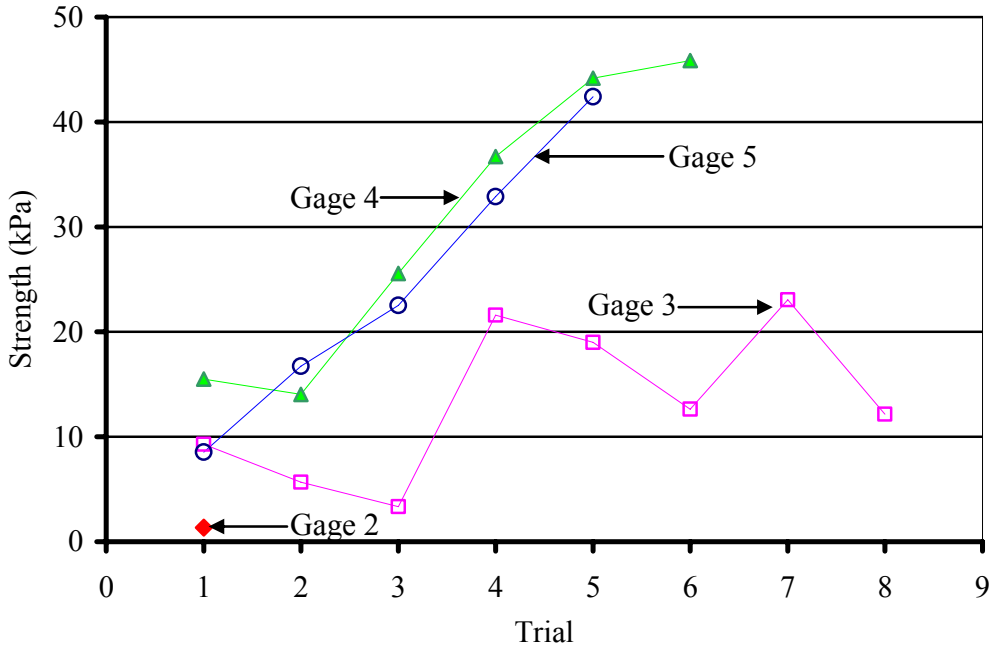

Figure 4.3 – Bond strength vs. bond test trial for plate WM-M-D

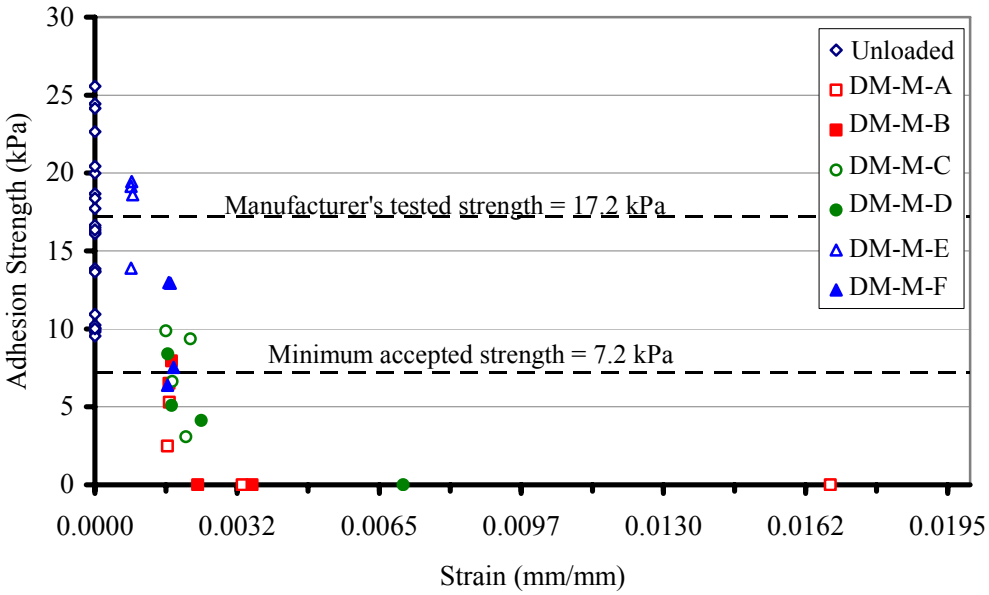

Figure 4.4 – Adhesive strength vs. steel strain at test location for DM-M plates

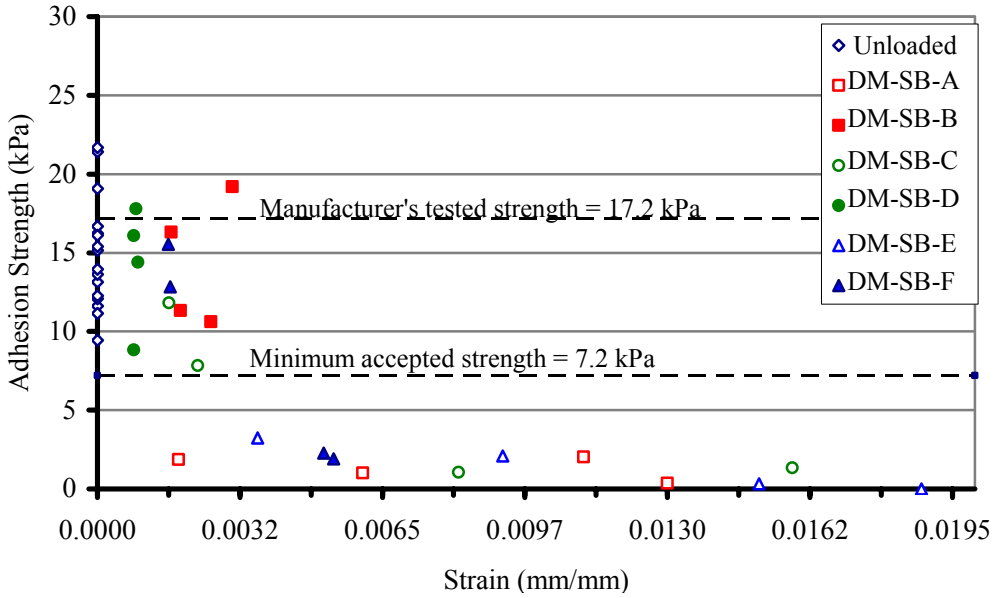

Figure 4.5 – Adhesive strength vs. steel strain at test location for DM-SB plates

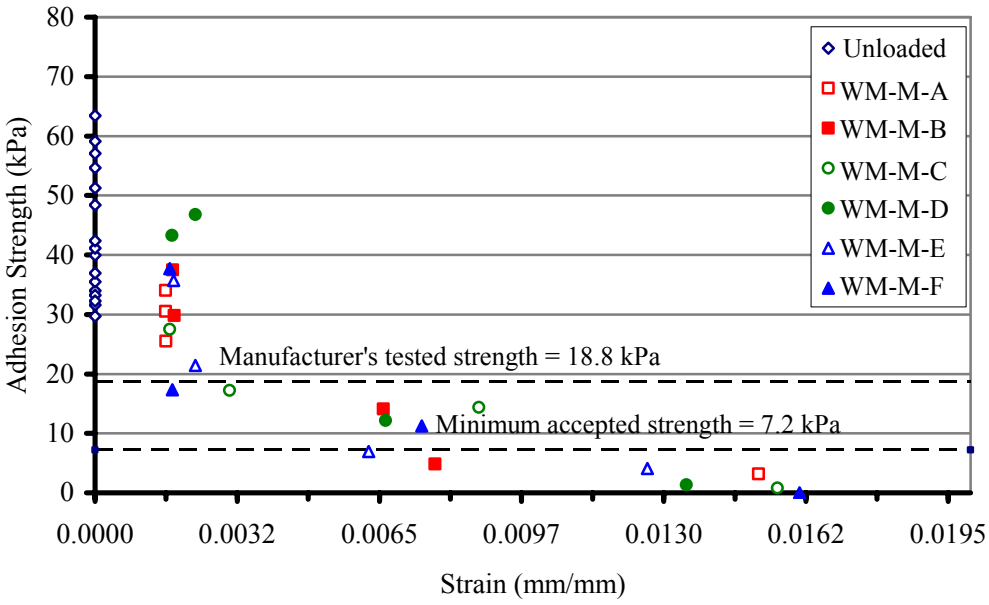

Figure 4.6 – Adhesive strength vs. steel strain at test location for WM-M plates

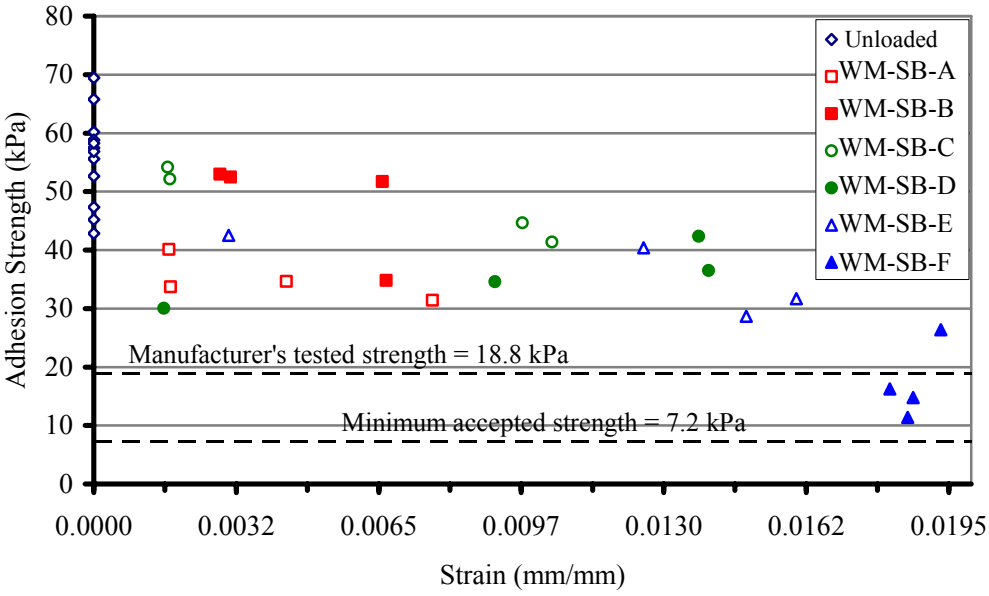

Figure 4.7 – Adhesive strength vs. steel strain at test location for WM-SB plates

(a) (b)

Figure 4.8 – DM behavior due to post-yield strain loading: (a) detachment of DM at one end; and (b) lack of adhesive strength after first cut is made into the DM

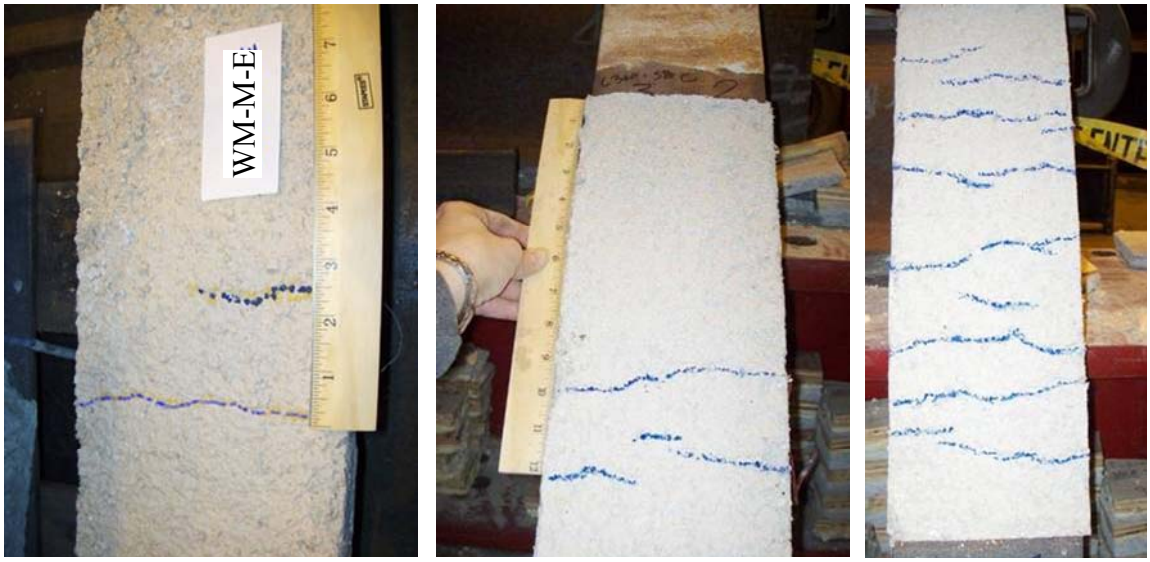

(a) (b) (c)

Figure 4.9 – Cracking in WM specimens: (a) typical WM-M specimen with one major and one minor crack; (b) plate WM-SB-C with minor additional cracking; and (c) plate WM-SB-F with extensive additional cracking

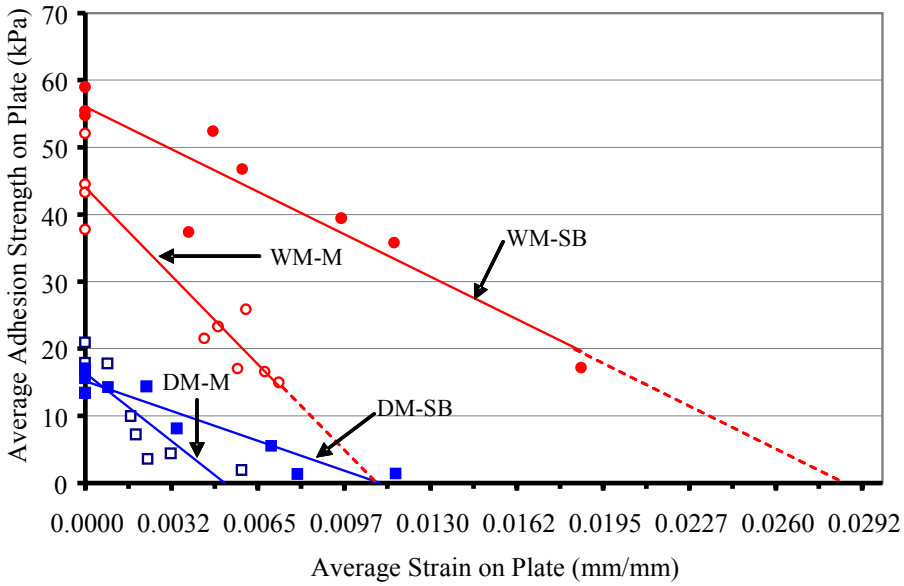

Figure 4.10 – Average adhesive strength on plates vs. average steel strain on plates

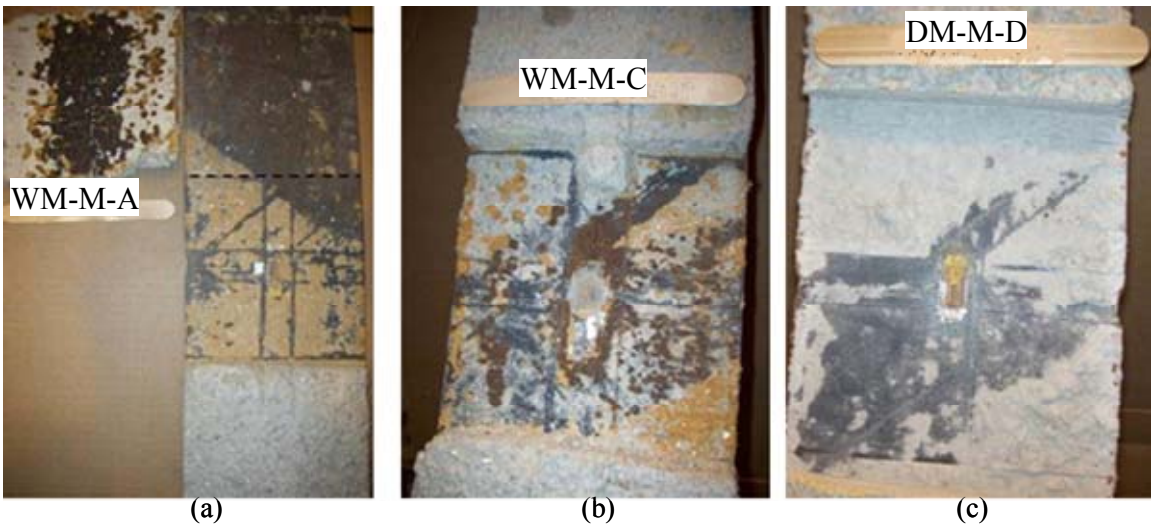

Figure 4.11 – Progression of yielding and loss of mill scale: (a) plate WM-M-A with detached SFRM at top, mill scale attached to SFRM, and diagonal yield lines; (b) plate WM-M-C with diagonal yield lines and loss of mill scale, but no detachment at edges of SFRM and; (c) plate DM-M-D showing yield lines and loss of mill scale

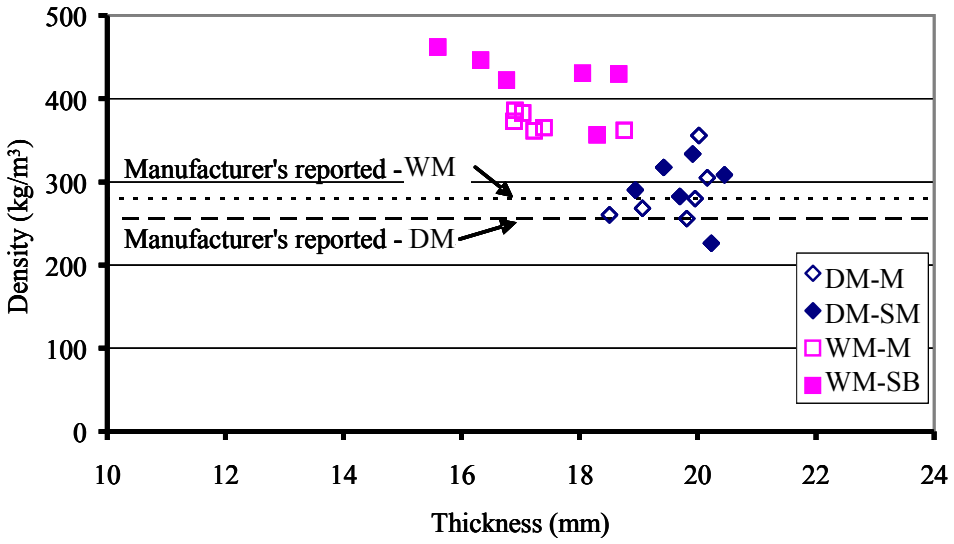

Figure 4.12 – Density vs. thickness for all plates tested

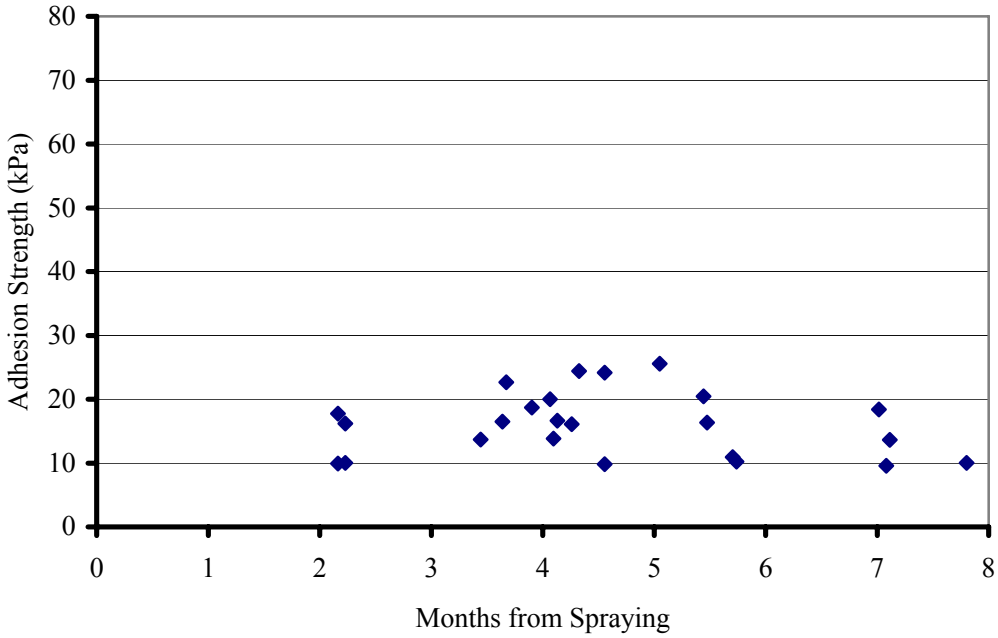

(a)

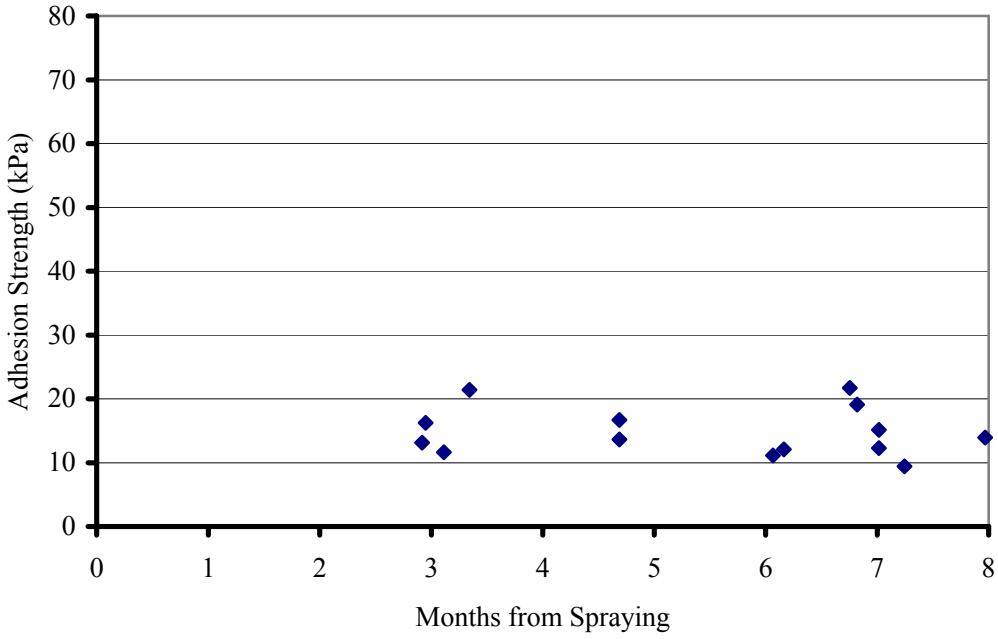

(b)

Figure 4.13 – Adhesive strength vs. age of unloaded plates: (a) DM-M; (b) DM-SB; [continued]

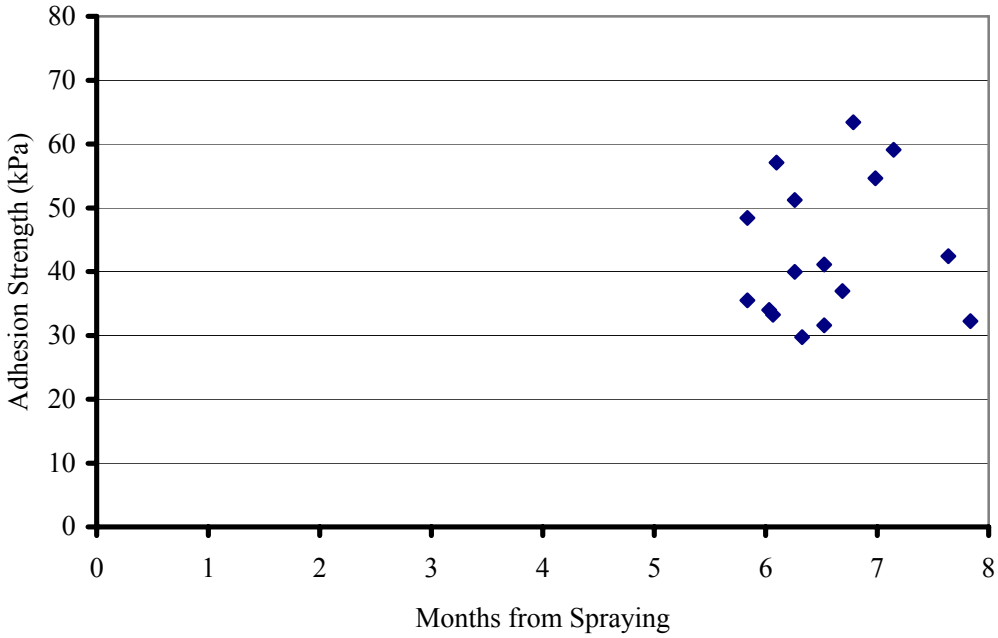

(c)

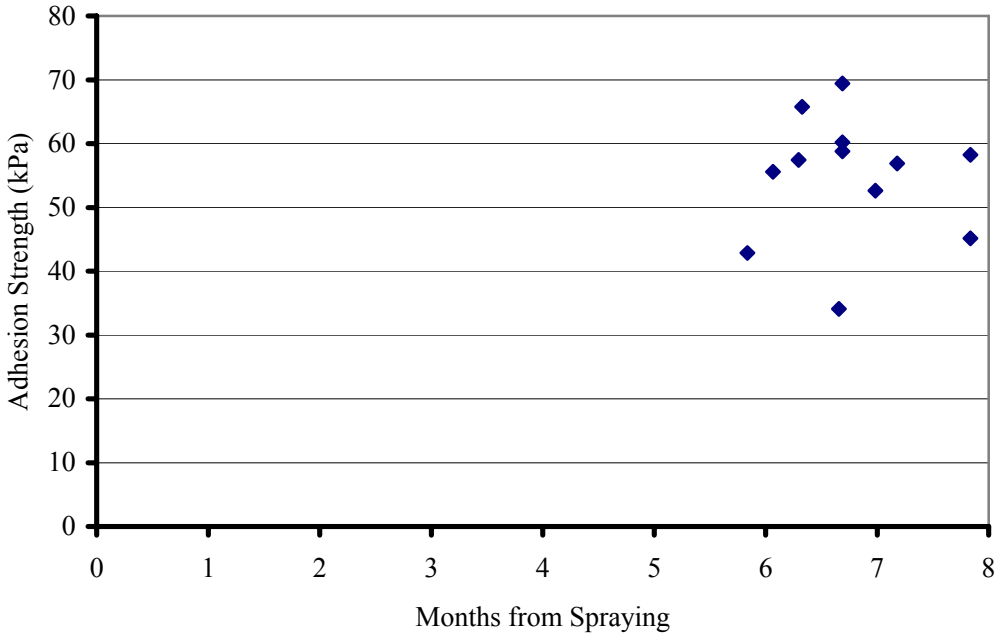

(d)

Figure 4.13 – [continued] Adhesive strength vs. age of unloaded plates: (c) WM-M; and (d) WM-SB

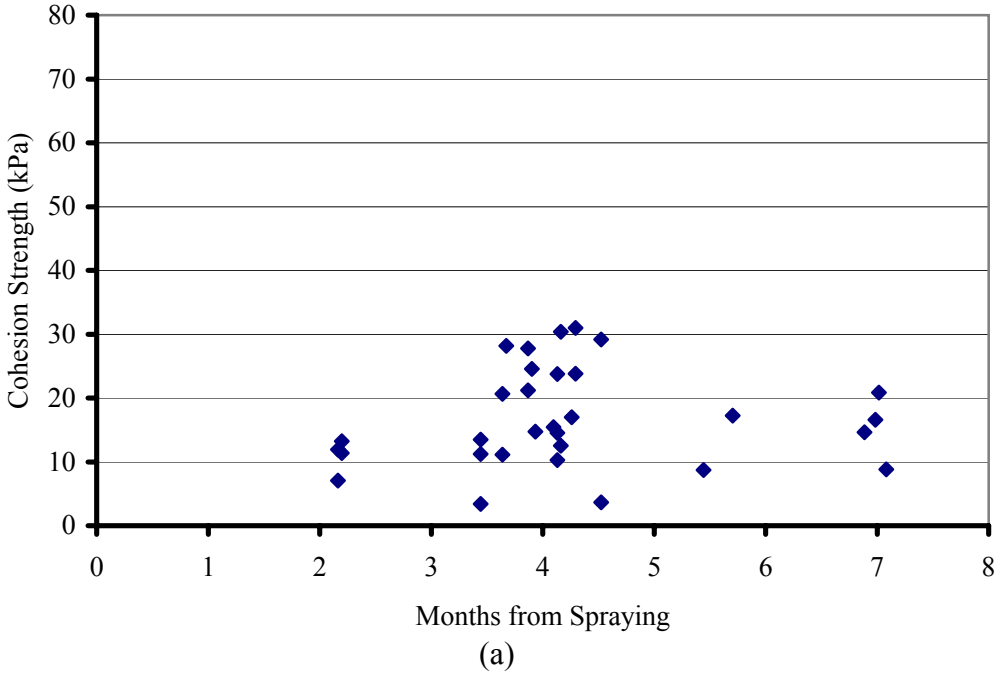

(a)

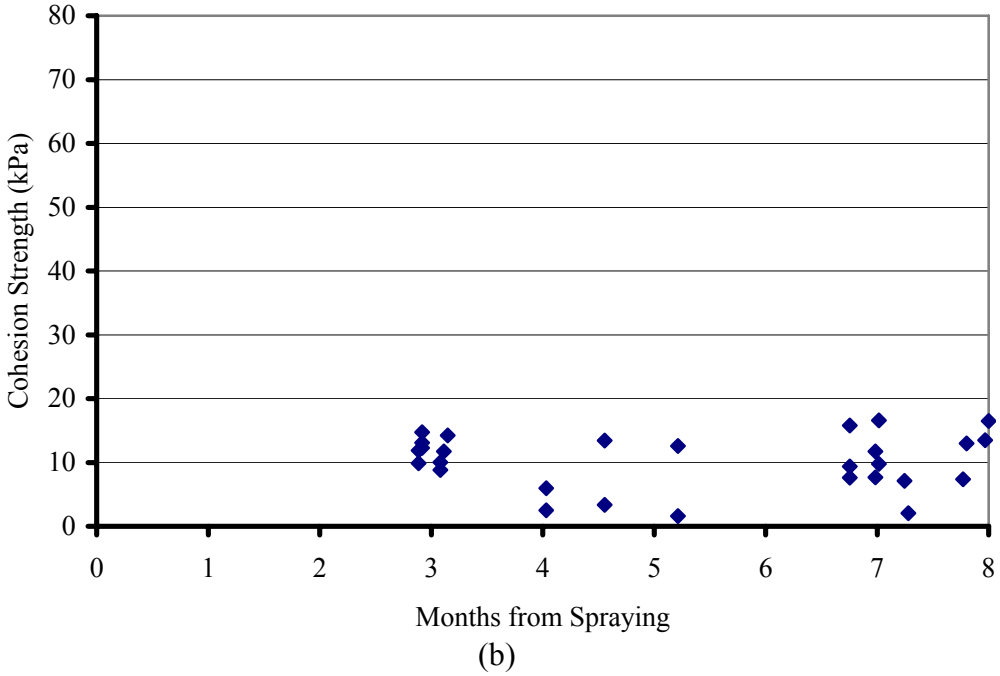

(b)

Figure 4.14 – Cohesive strength vs. age of unloaded plates: (a) DM-M; (b) DM-SB; [continued]

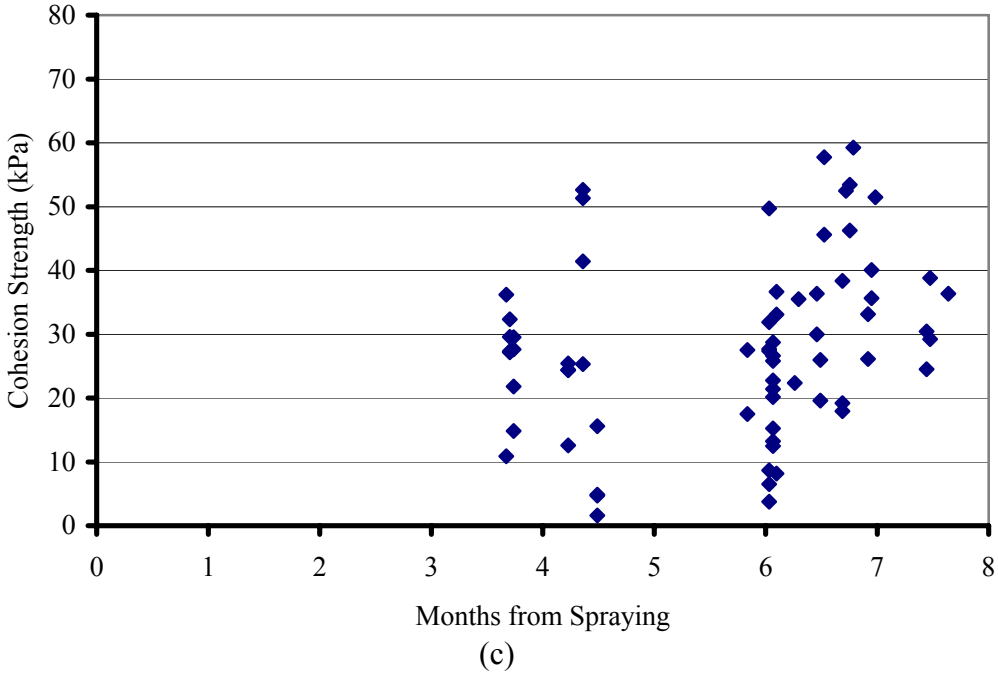

(c)

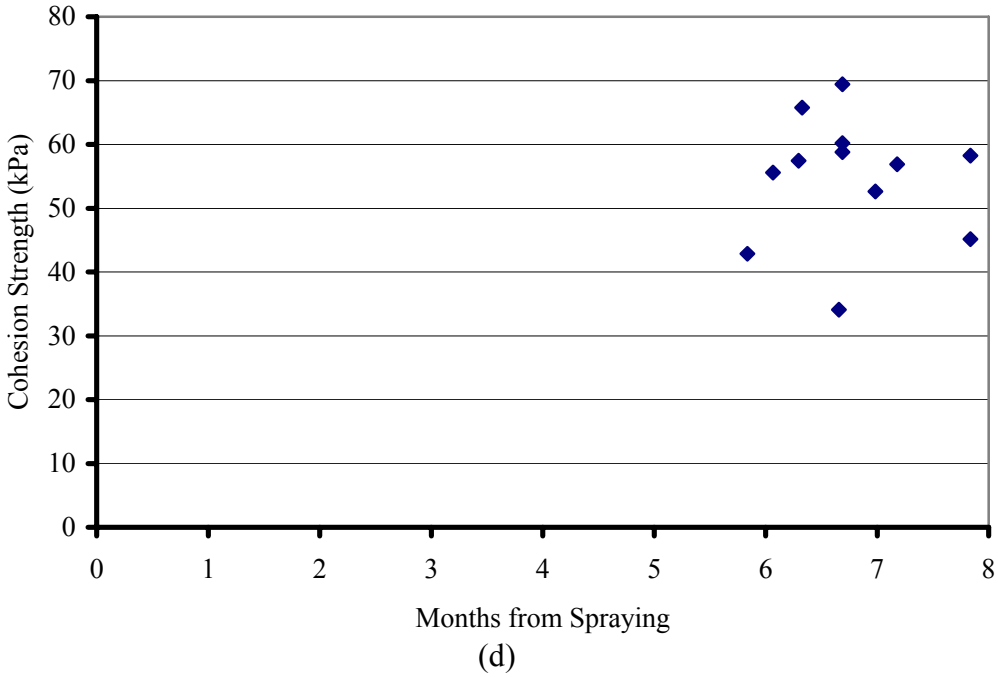

(d)

Figure 4.14 – [continued] Cohesive strength vs. age of unloaded plates: (c) WM-M; and (d) WM-SB

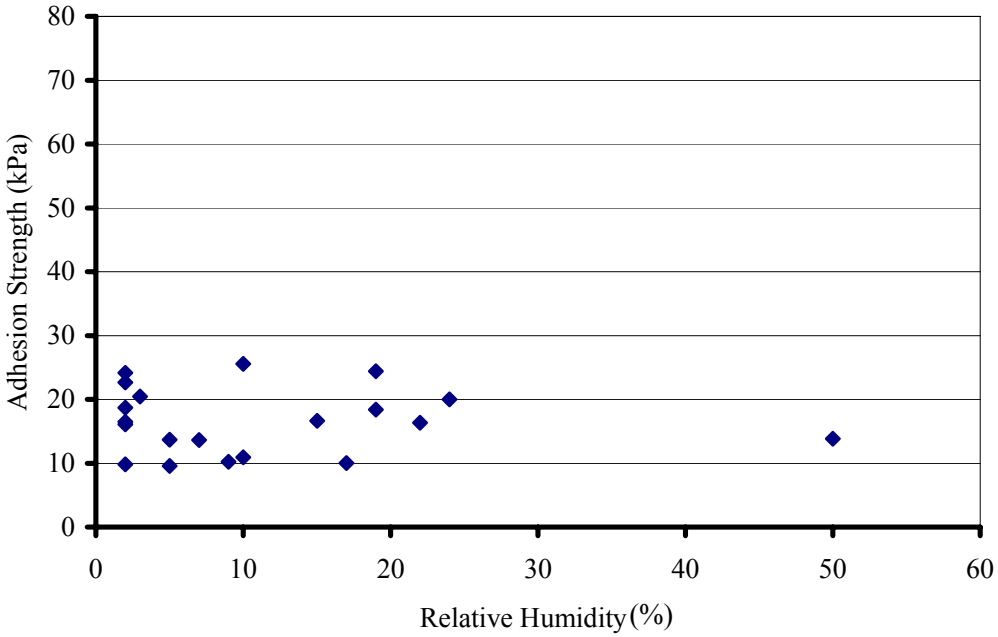

(a)

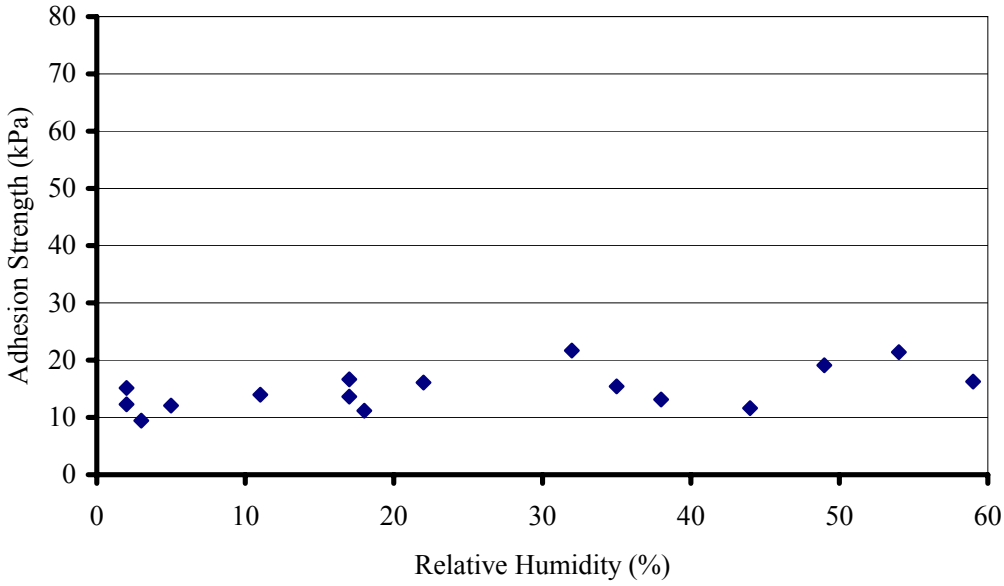

(b)

Figure 4.15 – Adhesive strength vs. relative humidity for plates: (a) DM-M; (b) DM-SB; [continued]

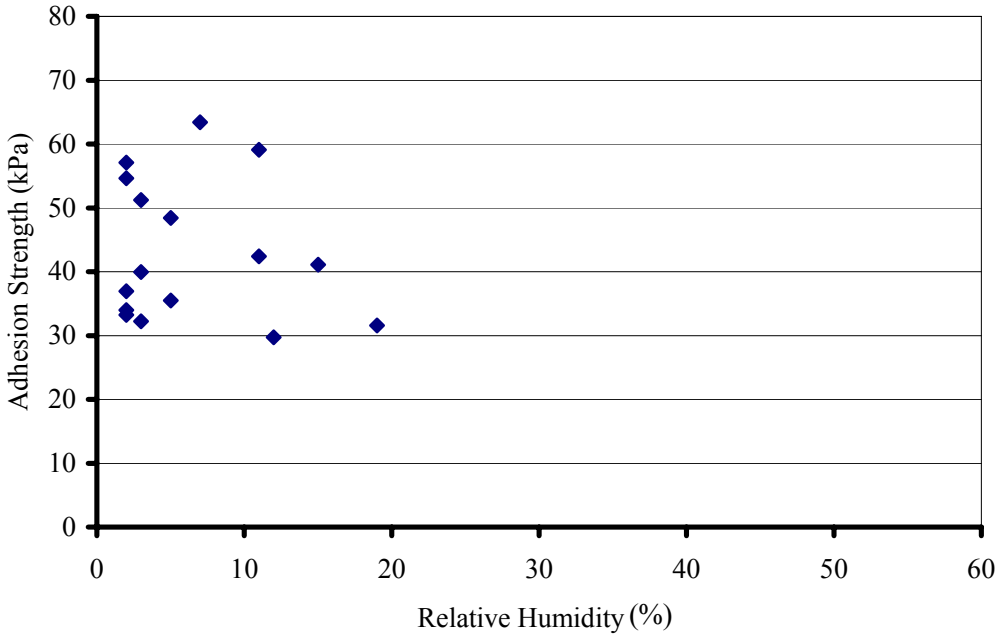

(c)

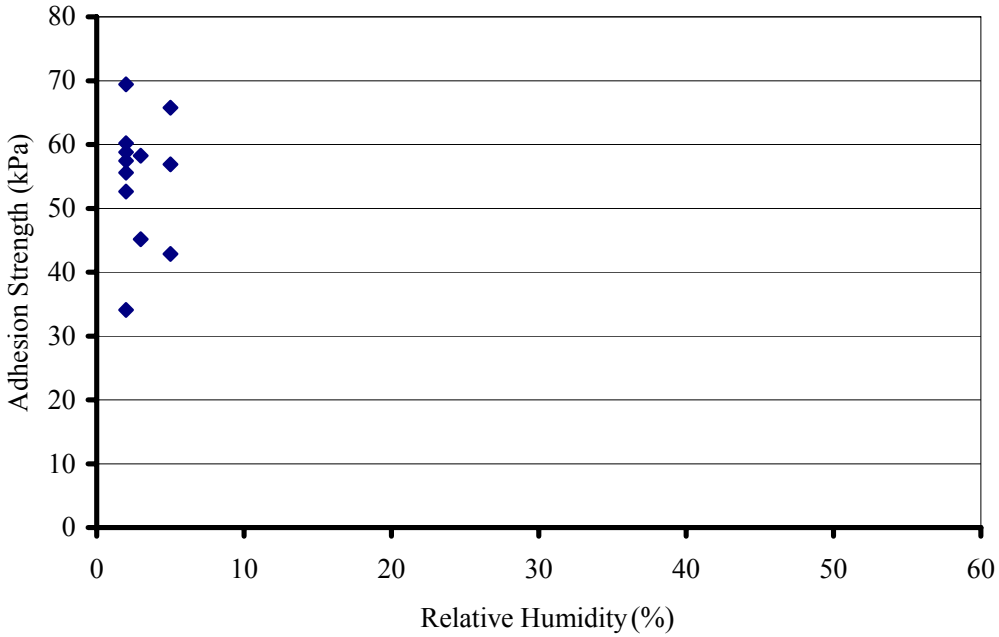

(d)

Figure 4.15 – [continued] Adhesive strength vs. relative humidity for plates: (c) WM-M; and (d) WM-SB

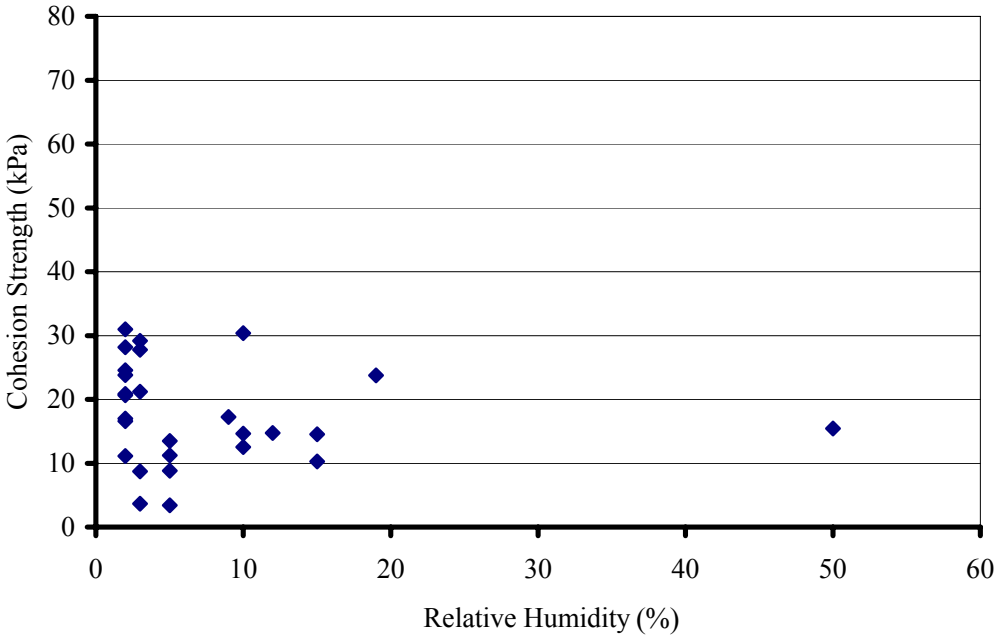

(a)

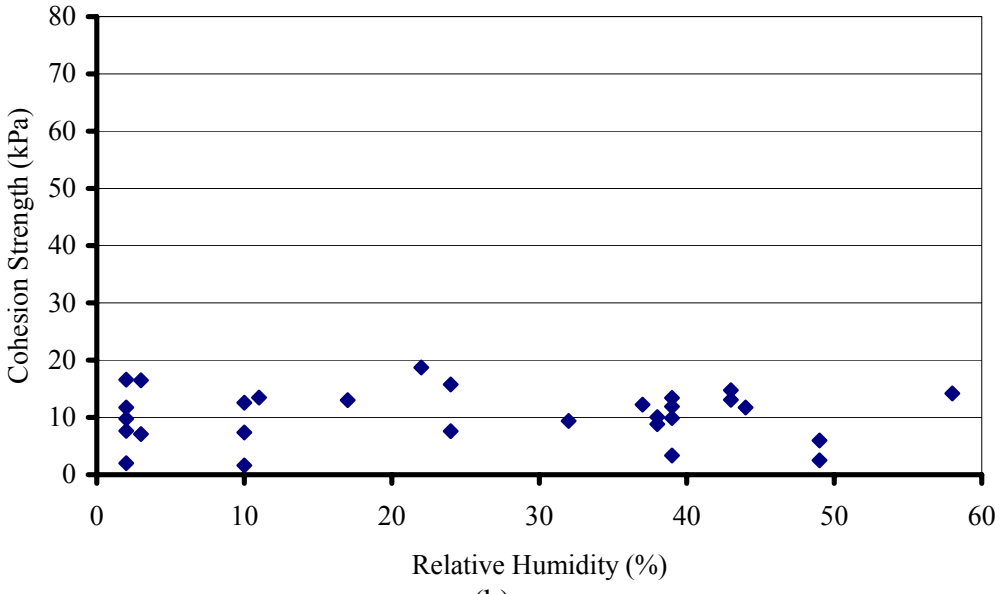

(b)

Figure 4.16 – Cohesive strength vs. relative humidity for plates: (a) DM-M; (b) DM-SB; [continued]

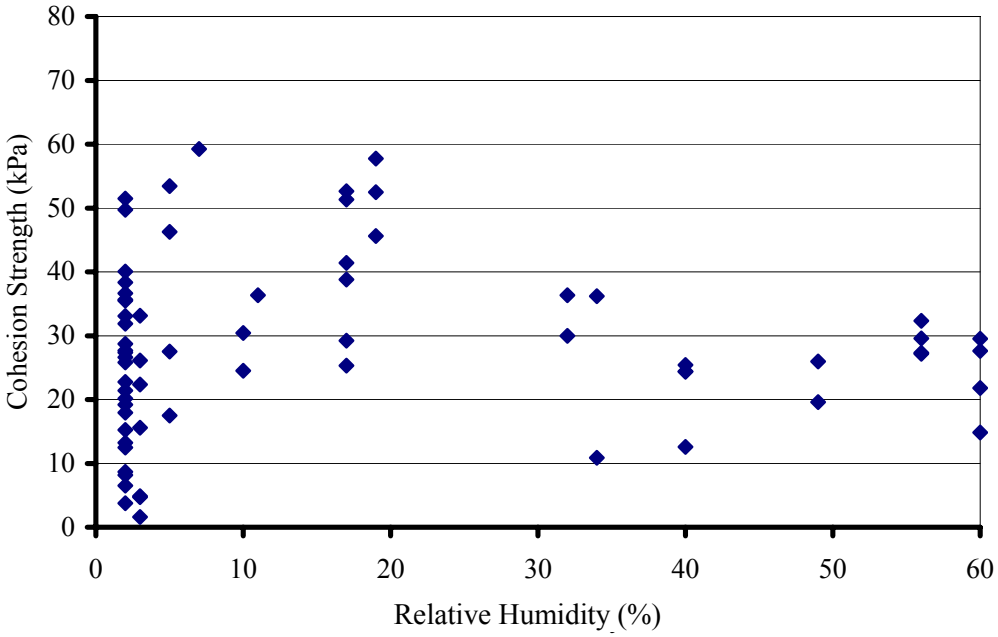

(c)

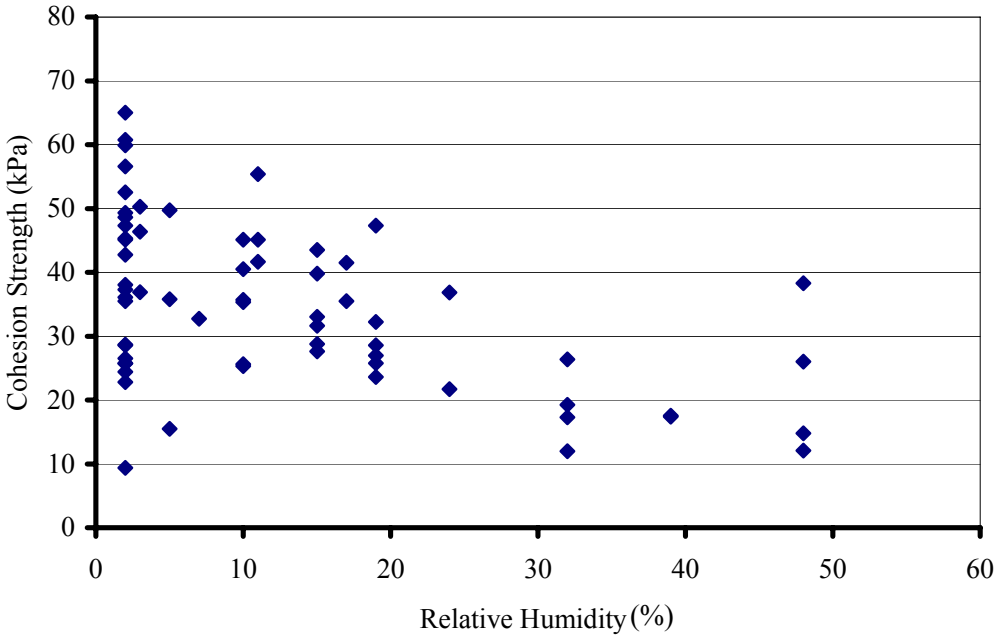

(d)

Figure 4.16 – [continued] Cohesive strength vs. relative humidity for plates: (c) WM-M; and (d) WM-SB

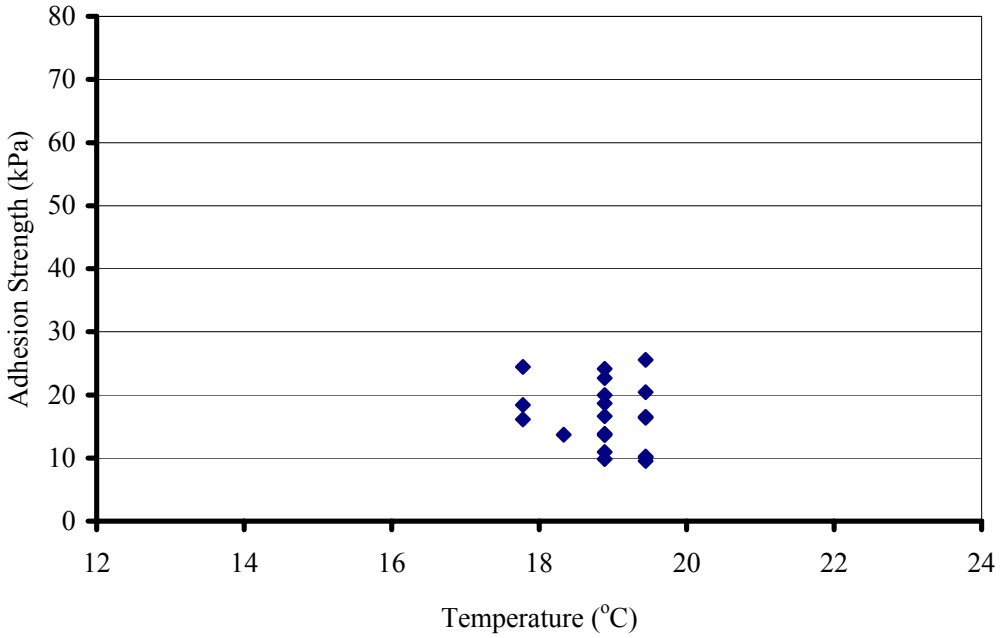

(a)

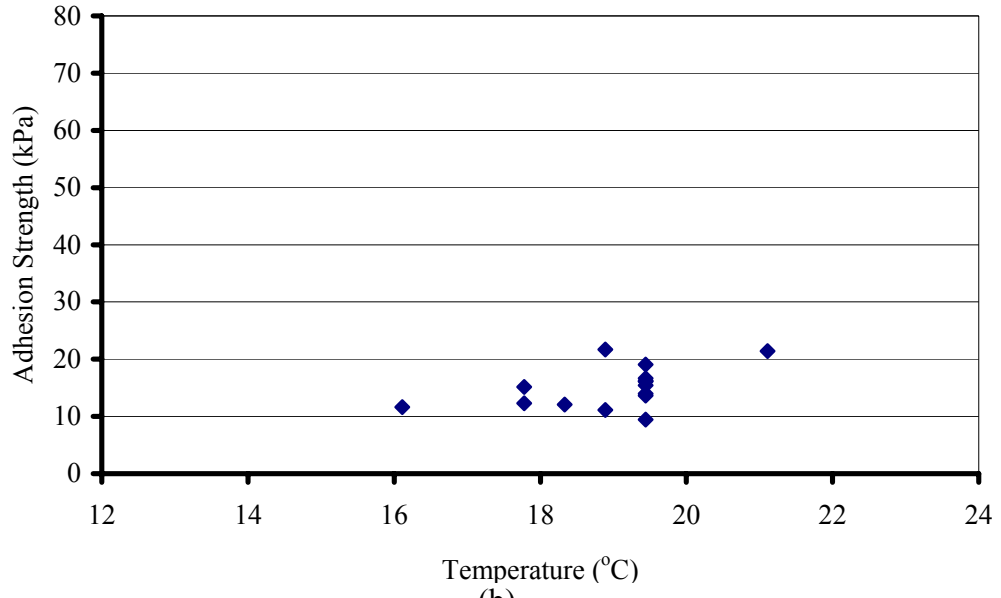

(b)

Figure 4.17 – Adhesive strength vs. ambient temperature for plates: (a) DM-M; (b) DM-SB; [continued]

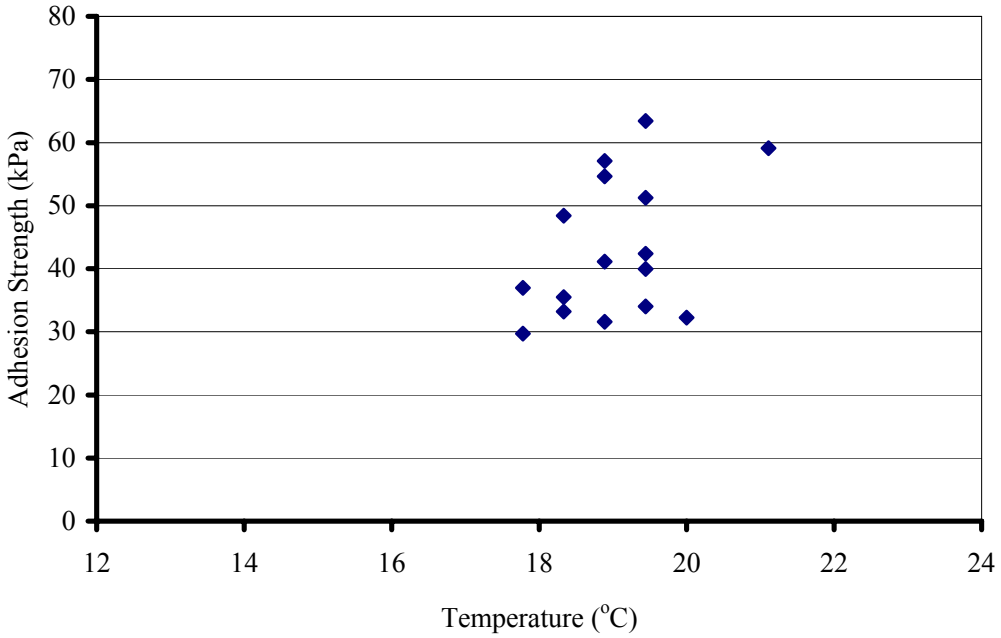

(c)

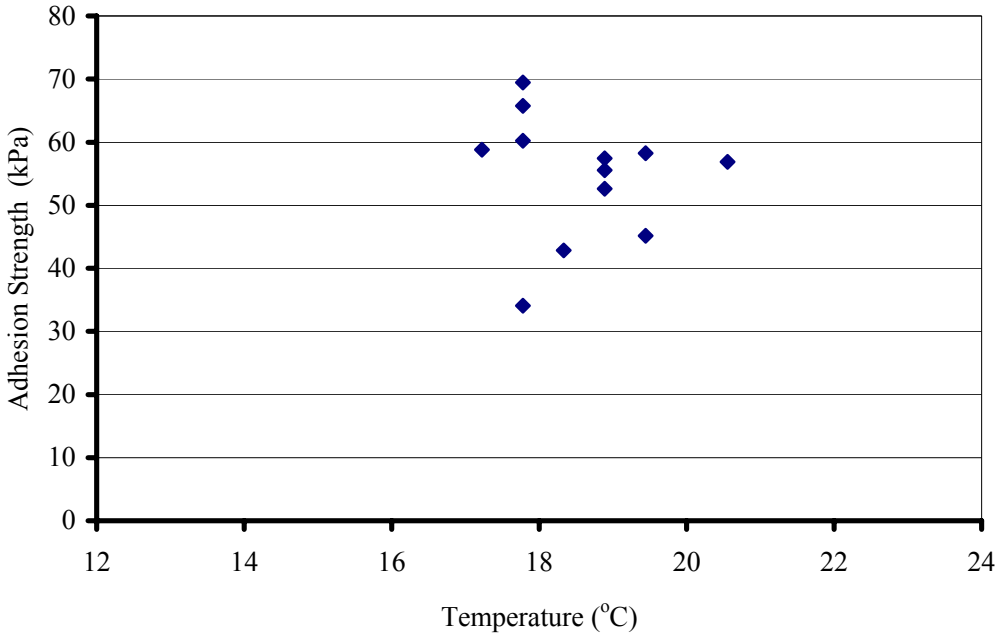

(d)

Figure 4.17 – [continued] Adhesive strength vs. ambient temperature for plates: (c) WM-M; and (d) WM-SB

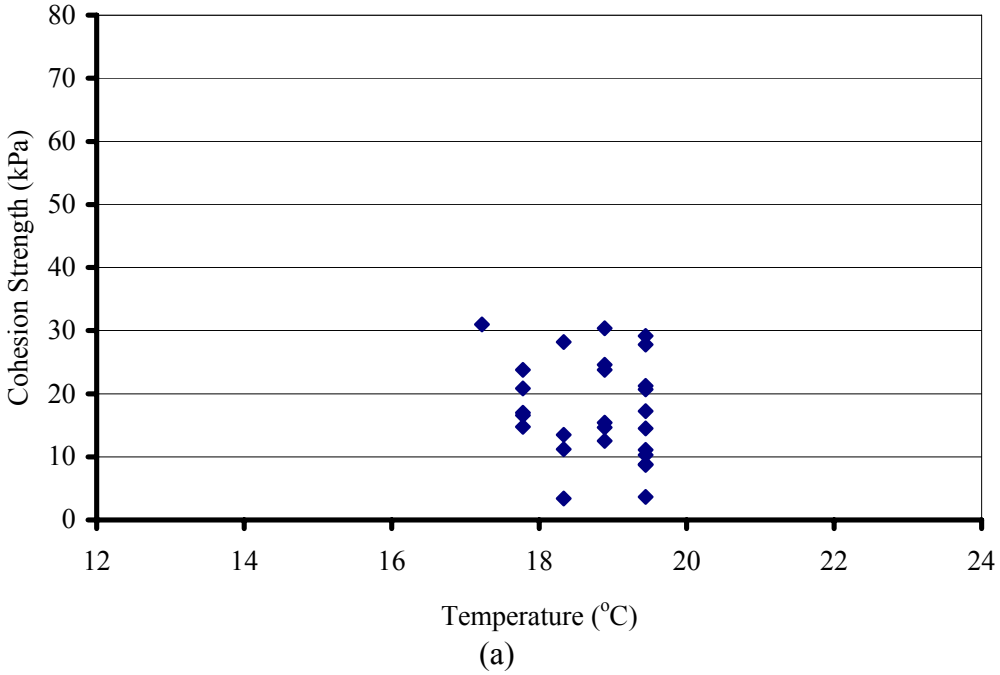

(a)

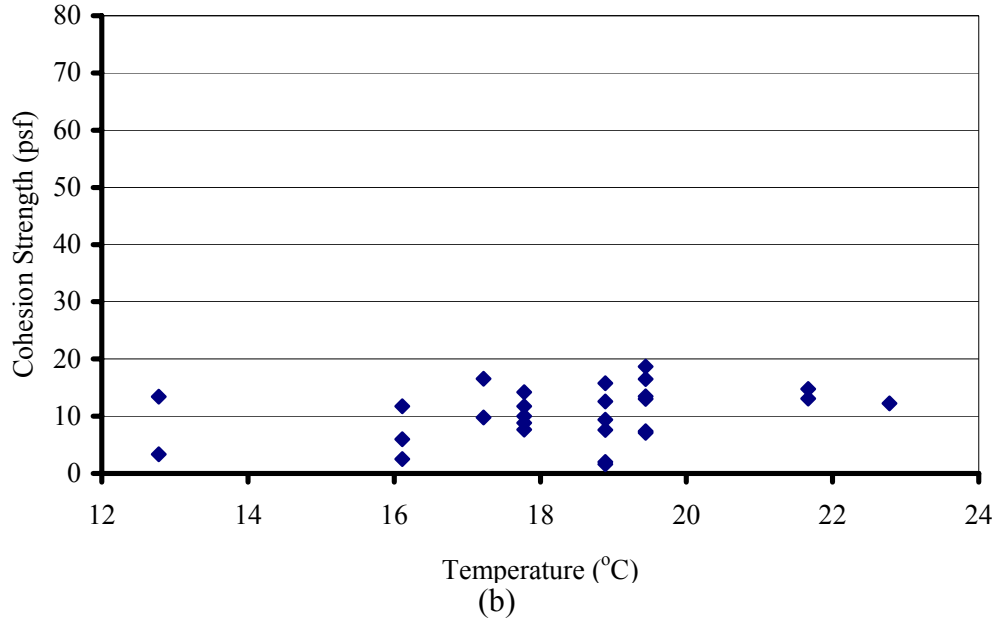

(b)

Figure 4.18 – Cohesive strength vs. ambient temperature for plates: (a) DM-M; (b) DM-SB; [continued]

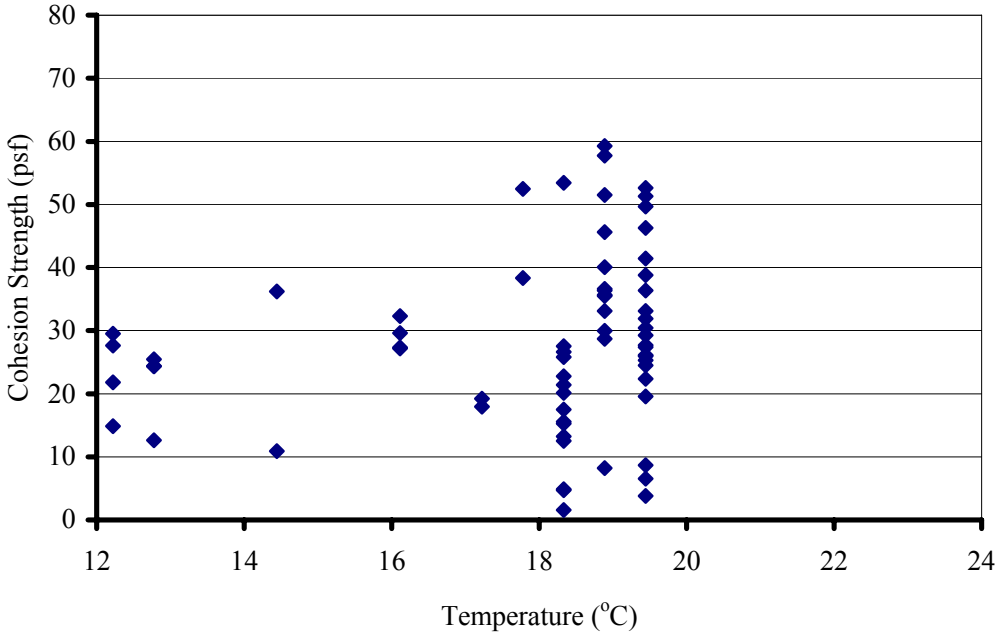

(c)

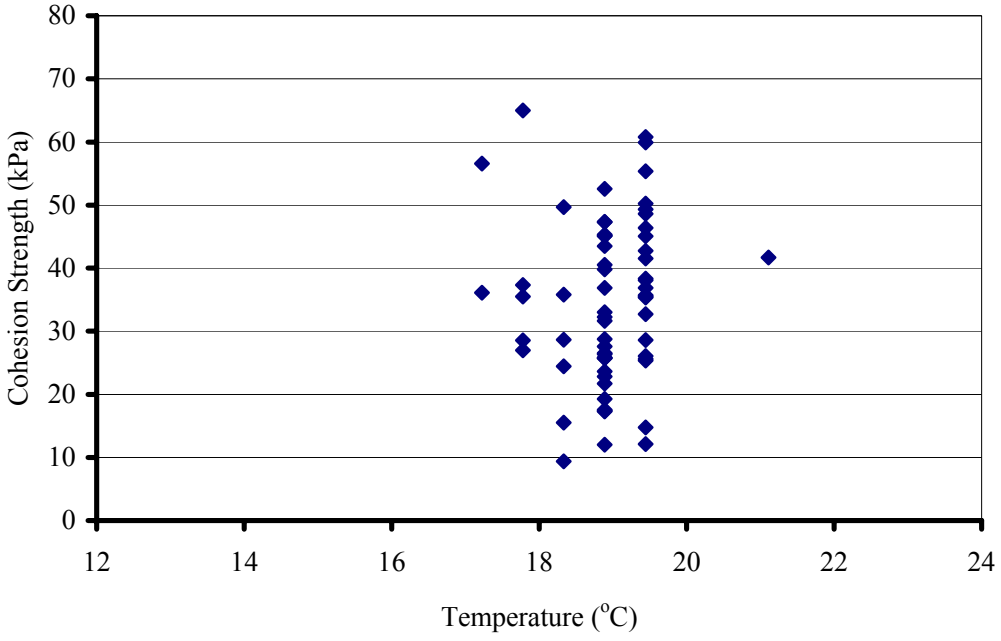

(d)

Figure 4.18 [continued] – Cohesive strength vs. ambient temperature for plates: (c) WM-M; and (d) WM-SB

CHAPTER 5
CONCLUSIONS

5.1 INTRODUCTION

The work presented in this report is part of a broader research program to evaluate the post-earthquake efficacy of sprayed fire resistive material (SFRM) in steel moment frame building structures.

This report focuses on tensile plate tests performed to examine the cohesive and adhesive strength of SFRM to steel at varying levels of strain, including beyond yield. SFRM was applied to a series of steel plates. The plates were then loaded in tension to various levels of strain above the yield strain. After loading, bond tests were performed on the SFRM to determine the adhesive and cohesive strengths of the SFRM as influenced by the tension tests. The test results were interpreted to understand the degradation of bond strength as a function of strain level in the steel substrate.

5.2 CONCLUSIONS

When the SFRM materials treated in this research are applied to steel that has mill scale, the adhesive strength of the SFRM degrades rapidly once the steel yields. The rapid degradation of the adhesive strength is attributed to the debonding of the mill scale from the steel as the steel yields, coupled with the fact that the SFRM is bonded to the mill scale and not the underlying steel.

WM has higher adhesive strength to steel than DM. Adhesive strength of WM on unloaded plates was about 3 times as great as the adhesive strength of DM on unloaded plates.

WM maintains bond to the steel at higher strain levels than DM. As was found in the visual inspections after the tension loading, the DM tends to debond from the steel surfaces while WM cracked but maintained the bond. This affect was first seen at the edges of the SFRM after loading, but the concept holds true for the central portion of the plate where bond tests were performed.

Sandblasting of the steel plates helps maintain adhesive strength to the steel at higher strain levels. Plates that were not sandblasted still had mill scale on the surface and once yielding progressed over the plate, the mill scale fell off effectively eliminating the bond between the steel and the SFRM.
Sandblasting of the steel plate increases unloaded adhesive strength in WM but does not offer this same advantage in DM.

SFRM may become detached from the steel plate after loading beyond yield. Detachment of the SFRM was more prevalent in the plates sprayed with DM than in the plates sprayed with WM. The fibrous DM tends to remain as one integral unit. When

strains become large and strain compatibility at the interface of the DM and the steel is lost, the DM debonds from the surface of the steel.

SFRM may crack after loading beyond yield. Cracking occurred in the WM but not in the DM. When strains become large and strain compatibility at the interface of the steel becomes difficult to maintain, the cementitous WM tends to crack to accommodate large deformations. The bond between the WM and the steel is strong and WM tends to detach from the steel at a lesser extent than DM does.

REFERENCES

Kohno, M., & Masuda, H. (2003). Fire-Resistance of Large Steel Columns under Axial Load, *Proceeding of the CIB-CTBUH International Conference on Tall Buildings*, Malaysia, pp. 95-102.

National Institute of Standards and Technology. (2005). *NCSTAR 1-3D: Mechanical Properties of Structural Steels*. Federal Building and Fire Safety Investigation of the World Trade Center Disaster. Washington, DC: US Government Printing Office, 288 pp.

National Institute of Standards and Technology. (2005). *NCSTAR 1-6A: Passive Fire Protection*. Federal Building and Fire Safety Investigation of the World Trade Center Disaster. Washington, DC: US Government Printing Office, 274 pp.

Standard Test Method for Cohesion/Adhesion of Sprayed Fire-Resistive Material (SFRM) Applied to Structural Members. (2000). ASTM Designation E736-00. West Conshohocken, PA: ASTM International.

Standard Test Method for Thickness and Density of Sprayed Fire-Resistive Material (SFRM) Applied to Structural Members. (2000). ASTM Designation E605-93. West Conshohocken, PA: ASTM International.

APPENDIX

A.1 Mill Certificate for Steel Plates

Steel Dynamics - Roanoke Bar Division
P.O. Box 13948 Roanoke, VA 24038
Office: 540-342-1831 Fax: 540-342-9437

Steel Dynamics®
Roanoke Bar Division

Test and Inspection Report NO. 35908-5
ROANOKE

KOONS STEEL, INC.
DAN BLANKLEY
PO BOX 476
PARKER FORD PA 19457-0476

Date 2/27/07

HEAT NUMBER	SIZE	1-YIELD Pt. KSI	ULTIMATE KSI	ELONG 8 IN.	BEND TEST	GRADE
JF6837	FLATS 1/4 X 6	47.1	67.3	32.5		A36
PURCHASE ORDER NUMBER	NUMBER PIECES	2-YIELD PT. KSI	ULTIMATE KSI	ELONG 8 IN.	BEND TEST	GRADE
29472	50 PIECES 20'	45.2	66.0	31.9		A36

HEAT NUMBER	SIZE	1-YIELD Pt. MPA	ULTIMATE MPA	ELONG 203mm	BEND TEST	GRADE
JF6837	FLATS 6.4 X 152.4	324.7	464.0	32.5		A36
PURCHASE ORDER NUMBER	NUMBER PIECES	2-YIELD PT. MPA	ULTIMATE MPA	ELONG 203mm	BEND TEST	GRADE
29472	50 PIECES 20'	311.6	455.1	31.9		A36

C	MN	S	P	SI	CR	NI	MO	CU	V	NB
.13	.77	.025	.010	.23	.07	.08	.01	.34	.004	.002

Commonwealth of Virginia
Sworn to and subscribed before me this 2nd day
March 2007 Witness my hand and official seal.
, Notary Public

MERCURY, RADIUM OR OTHER ALPHA SOURCE MATERIALS IN ANY FORM HAVE NOT BEEN USED IN THE PRODUCTION OF THIS MATERIAL. NO WELD REPAIR HAS BEEN PERFORMED.

My commission expires April 30, 2010

Approved ABS QA Mill. Certificate No. 00NN10108-X.

This material was melted and manufactured in the USA by basic Electric Furnace processes to meet specification: ASTM A36-04 ASME SA36 QQS741D A709-00A GR36 AASHTO M270 GR 36 IMPACTS WAIVED

The tensile values stated in either inch-pound units or SI units are to be regarded as separate as defined in the ASTM scope for this material. Unless a metric specification is ordered, this material has been tested and meets the requirements of the inch-pound ranges.

This is to certify the above to be a true and accurate report as contained in the records of this company.

Engineer of Tests: Charles R. Charlton